



# Chitosan as an Environmentally Friendly Corrosion Inhibitor—A Review

Atanu Kumar Das<sup>1,2</sup> · Md. Nazrul Islam<sup>3</sup> · David A. Agar<sup>1</sup> · Roni Maryana<sup>4</sup> · Magnus Rudolfsson<sup>1</sup>

Received: 27 February 2025 / Revised: 13 August 2025 / Accepted: 21 November 2025  
© The Author(s) 2025

## Abstract

Corrosion poses a significant challenge for industries such as automotive, marine, construction, and oil and gas, as it impacts the production of high-quality goods while keeping maintenance costs low. Corrosion reactions, including oxidation and reduction on metal surfaces, can be mitigated using corrosion inhibitors. Traditionally, chromate and phosphate-based compounds have been employed in various sectors to prevent these reactions. However, concerns about their toxicity and environmental impact have spurred the search for non-toxic alternatives. Chitosan (CT), a biodegradable and renewable material derived from chitin, shows promise as a corrosion inhibitor due to its film-forming ability and antimicrobial properties. Its hydroxyl and free amino groups enhance its effectiveness in various corrosive environments, making CT suitable for protecting metals across different industries. Previous research has explored the use of CT-based composites and standalone CT materials as coatings on metal surfaces. Both types have also been tested directly in corrosive environments, demonstrating promising results for protecting various metals from corrosion in different corrosive media. This review article aims to investigate the application and mechanism of CT as a corrosion inhibitor. It discusses the preparation methods, application techniques, and performance of CT as an anticorrosive material, concluding with an explanation of its corrosion inhibition mechanism. This review is intended to enhance researchers' understanding of CT's potential in corrosion inhibition and support its further development as an effective corrosion inhibitor.

**Keywords** Chitosan · Metal corrosion · Corrosive media · Corrosion inhibition

## 1 Introduction

---

✉ Atanu Kumar Das  
atanu.kumar.das@ri.se; atanufwt03ku@yahoo.com  
Md. Nazrul Islam  
nazrul17@yahoo.com  
David A. Agar  
david.agar@slu.se  
Roni Maryana  
roni.maryana@gmail.com  
Magnus Rudolfsson  
magnus.rudolfsson@slu.se

<sup>1</sup> Department of Forest Biomaterials and Technology, Swedish University of Agricultural Sciences, 90183 Umeå, Sweden

<sup>2</sup> Cellulose Technology, Department of Sustainable Materials and Packaging, RISE Research Institutes of Sweden, Hörneborgsvägen 10, Domsjö, 892 50 Örnsköldsvik, Sweden

<sup>3</sup> Forestry and Wood Technology Discipline, Khulna University, Khulna 9208, Bangladesh

<sup>4</sup> Research Center for Chemistry, Indonesian Institute of Sciences, Serpong, Tangerang Selatan, Banten, Indonesia

Corrosion presents significant challenges across various industries, including maritime, oil and gas, automotive, and construction. It typically results from an electrochemical reaction between metal and its environment [1], involving oxidation processes that must be managed to protect the metal from deterioration [2, 3]. Effective corrosion inhibition strategies are crucial for ensuring high-quality production and reducing maintenance costs [4]. The service life of industrial metallic surfaces can be extended through the use of effective corrosion inhibitors [5]. However, the effectiveness of these inhibitors varies based on environmental conditions and the type of metal involved [6]. While chromate-based corrosion inhibitors are highly toxic to the environment [4], zinc-based inhibitors can be harmful to certain aquatic organisms [6]. Conversely, phosphate-based anticorrosive materials can encourage biological growth [6]. Consequently, researchers have called for the development of new organic-based anticorrosive materials [4, 6].

Renewable and biodegradable corrosion inhibitors made from low-cost materials are being explored for industrial applications [4]. Biomaterial-based organic corrosion inhibitors possess valuable properties, including antioxidant, anti-inflammatory, anti-fungal, anti-cancer, anti-viral, and anti-microbial effects [7]. These inhibitors can create a physical barrier between metal surfaces and their environments, effectively protecting against corrosion [8, 9]. The use of organic-based corrosion inhibitors is both cost-effective and environmentally friendly [10–12]. Chitosan (CT), a natural biomaterial derived from chitin, is particularly significant due to its abundance, being the second most common biopolymer on Earth, after cellulose. Chitin is a structural component found in the exoskeletons of crustaceans (such as shrimp, crabs, and lobsters), insects, and the cell walls of fungi [13]. CT exhibits unique characteristics, including biodegradability, anti-microbial activity, film-forming ability, and biocompatibility [14]. Its rich hydroxyl and free amino groups enhance its appeal in anti-corrosion applications. Consequently, CT shows great potential for protecting metals against various corrosive media [5, 15–29].

CT-based inhibitors can be utilized as either standalone materials [30–32] or as part of composite materials [33, 34]. Both forms can be applied as coatings on metal surfaces [31–34] or in conjunction with corrosive media [35–38] to prevent metal corrosion. The differing application processes of CT-based anticorrosive materials result in varied anti-corrosion mechanisms. Previous studies have predominantly focused on their application to specific metals, with only a limited number investigating CT's use in steel alloys [5] and aluminum alloy 2024 [14]. These authors discussed the effectiveness of CT-based corrosion inhibitors in relation to specific metals, while Verma et al. [39] discussed specific CT-based Schiff bases for corrosion inhibition. However, no single study has comprehensively addressed all aspects of CT as a corrosion inhibitor, including preparation methods and application techniques. Furthermore, their performance across different metal types has not been thoroughly evaluated. A consolidated overview of CT-based corrosion inhibitors would benefit both academia and industry by highlighting current knowledge and guiding future developments in this field.

This study provides an overview of the implications of CT-based corrosion inhibitors for various metals. It details the preparation and application processes, including coating

and mixing with corrosive metals, as well as the functionality and mechanisms of these inhibitors. The paper begins with a general introduction to CT and concludes with recommendations for necessary improvements suggested in scientific documents published until the end of 2024 in this field.

## 2 Chitosan

CT, a semi-synthetic biopolymer derived from chitin—the second most abundant biopolymer on Earth [40]—appears as white and yellow flakes. Its molecular structure features  $\alpha$ -1,4-linked 2-amino-2-deoxy- $\alpha$ -D-glucose (N-acetyl glucosamine) (Fig. 1) [41]. The molecular weight of CT, which averages around  $1.2 \times 10^5$  g mol $^{-1}$ , is influenced by the intensity of deacetylation [42]. While CT is insoluble in water [43], it can dissolve in organic acid solutions such as formic and acetic acid at a pH below 6.0 [44]. This solubility is contingent upon a deacetylation degree of at least 85% [43]. Additionally, CT is non-toxic and biodegradable, making it suitable for various applications [45].

## 3 Preparation of Chitosan-Based Corrosion Inhibitor

CT has reacted with various compounds to create composites that serve as corrosion inhibitors. It has also been blended with other active compounds for use as anti-corrosive agents. Additionally, with some modifications, CT has been utilized independently. This section outlines the preparation methods for corrosion inhibitors based on CT, with an overview presented in Fig. 2.

### 3.1 Chitosan-Based Composites

Chitosan, its functionalized forms, and its nanoparticle composites are widely recognized as effective corrosion inhibitors for various metal and medium systems. A diverse array of materials has been utilized to prepare CT-based composites for corrosion inhibition. Researchers have blended CT with other compounds to assess their corrosion inhibition efficiency. General information on CT-based corrosion inhibitors, their applications, and the corrosive media involved is summarized in Table 1.

Silver nitrate ( $\text{AgNO}_3$ ), the most affordable silver salt, offers antiseptic and non-hygroscopic properties. CT is combined with silver nitrate to create a CT/ $\text{AgNO}_3$ -based anticorrosive nanocomposite [6]. Additionally, silver nanoparticles (AgNPs) have been employed to develop CT/AgNPs nanocomposites. To produce these composites,

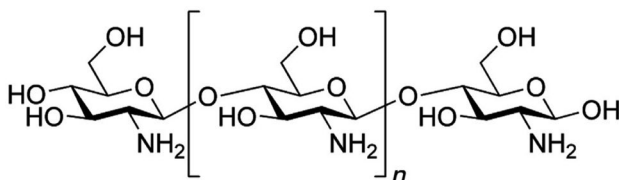
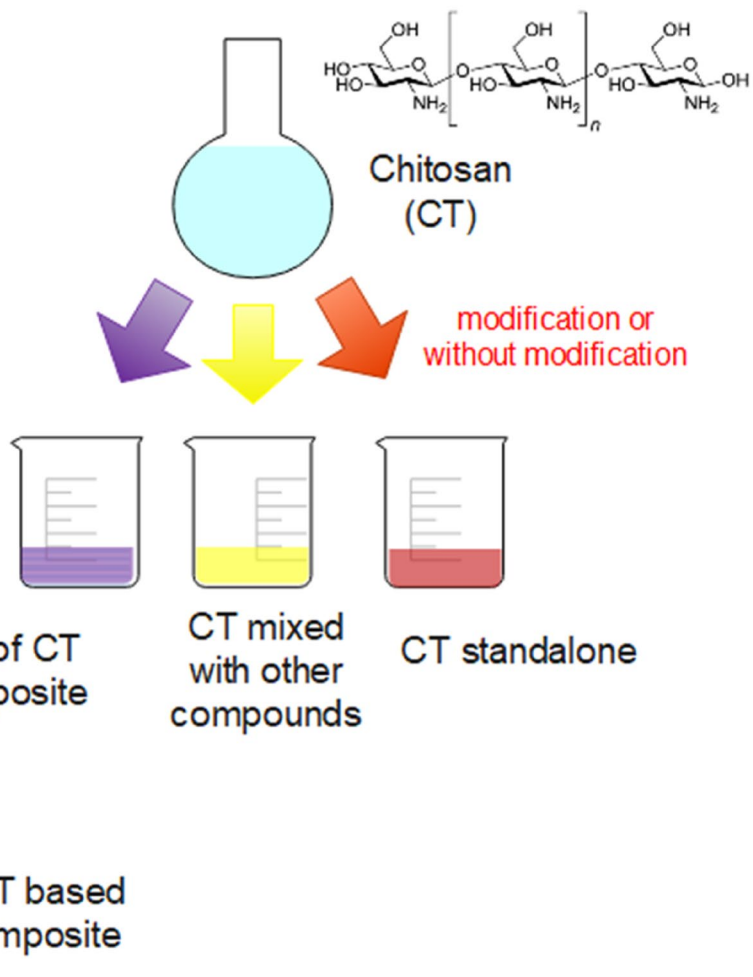


Fig. 1 Chemical structure of chitosan [41]

**Fig. 2** Preparation of CT-based corrosion inhibitor



AgNPs and a CT solution are prepared by dissolving them in water and acetic acid ( $\text{CH}_3\text{COOH}$ ), respectively. The two solutions are then mixed, and honey is added to synthesize the CT/AgNPs composite. In another study, anionic CT surfactant was synthesized through the reaction of a CT solution with 2-formylbenzenesulfonic acid sodium salt, followed by esterification, drying, and crystallization using diethyl ether. This anionic CT surfactant was then reacted with AgNPs via a photochemical reduction method using sunlight to obtain the CT/AgNPs composite [46].

Researchers have utilized silica ( $\text{SiO}_2$ ) and cerium oxide ( $\text{CeO}_2$ ) nanoparticles to create CT-based nanocomposite corrosion inhibitors. Bahari et al. [47] dissolved 2-mercaptobenzothiazole (MBT) in a  $\text{CH}_3\text{COOH}$  solution containing CT. They then mixed ethanol-washed  $\text{SiO}_2$  nanoparticles with the CT/MBT solution and added glutaraldehyde (GA) to yield the CT/MBT/ $\text{SiO}_2$ /GA corrosion inhibitor. For the CT/ $\text{CeO}_2$  nanocomposite, CT was first dissolved in  $\text{CH}_3\text{COOH}$ , then precipitated with acetone and dried. This was followed by re-dissolving it in an acidified NaCl medium to produce a CT hydrogel, into which nano  $\text{CeO}_2$  was dispersed.

In another study, Pitakchatwong et al. [48] developed CT-based nanocapsules, with or without MBT, using an oil-in-water emulsion process. Initially, they prepared Schiff bases of CT with 3-nitrosalicylic acid (3NiSA) to prepare two composites: CT-3NiSA-S and CT-3NiSA with amide bond (CT-3NiSA-A). They then transformed these into nanocapsules through emulsification, sonication, crosslinking, and maintaining an inert atmosphere with nitrogen. For MBT-loaded nanocapsules (CT-3NiSA-S-MBT or CT-3NiSA-A-MBT), they emulsified the mixture similarly, adding MBT.

Additionally, Santos et al. [49] prepared the CT/ $\text{SiO}_2$  capsule through the hydrolysis and polycondensation of tetraethoxysilane (TEOS) in the presence of CT. They added benzotriazole and polysorbate 80 to CT dissolved in  $\text{CH}_3\text{COOH}$  under controlled temperature, followed by TEOS and emulsification using an oil-in-water process. An  $\text{NH}_4\text{OH}$  solution dispersed in mineral oil was then added to this emulsion, which was subsequently centrifuged and dried to yield the SiCTBSEG composite. This composite was calcined to produce SiCTBSEG-cal.

Moreover, thiocarbohydrazide (TC) was employed to produce TC/CT-based corrosion inhibitors. In this case, TC

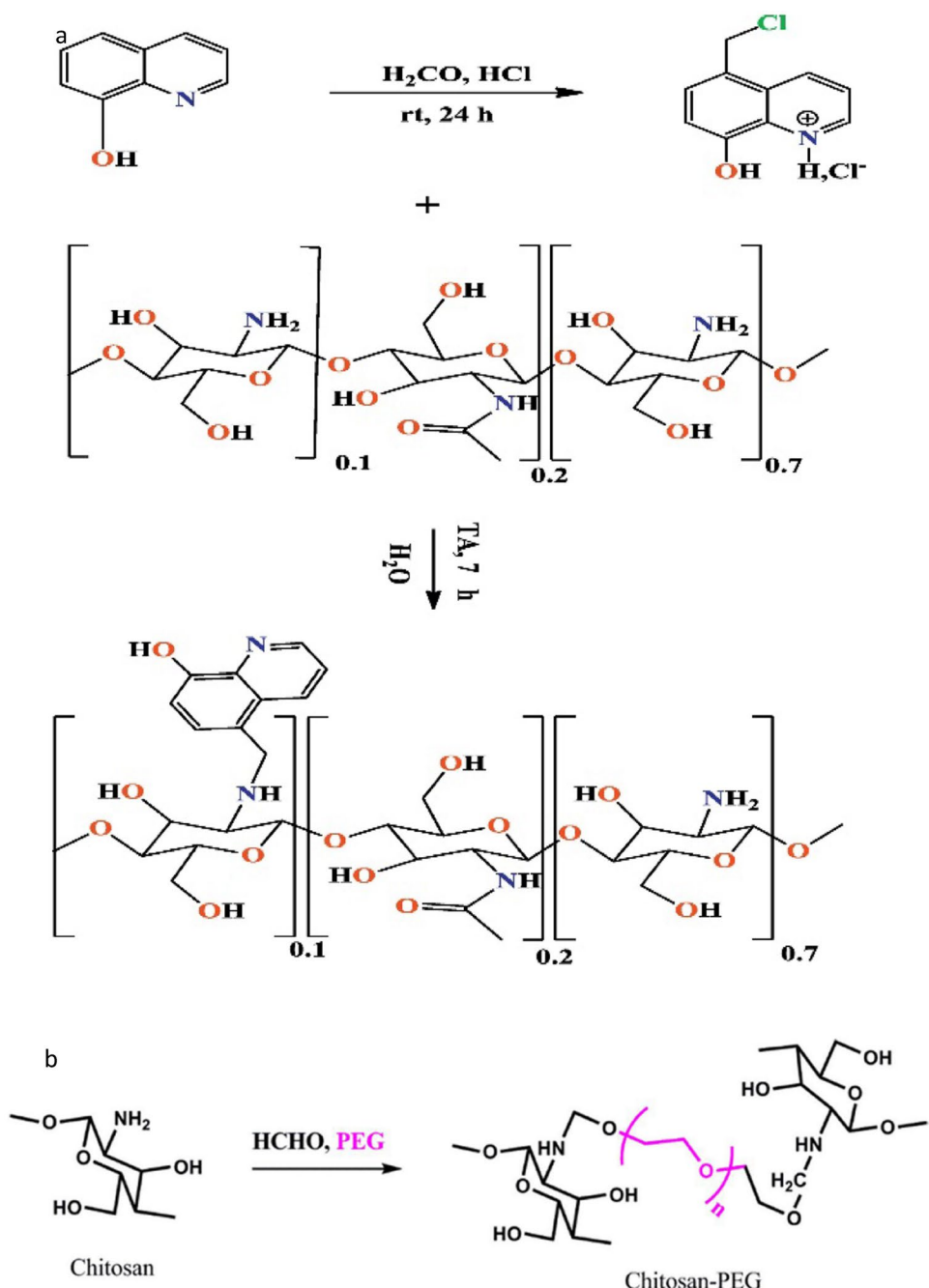
**Table 1** A general overview of chitosan-based corrosion inhibitor (summarized based on the literature discussed in this study)

Inhibitor type	Application type	Substrate type	Corrosive media	Performance
CT-based composites	Coating	Copper	NaCl	Improved corrosion inhibition efficiency
CT with nano $\text{Fe}_2\text{O}_3$ , CT/ $\text{Na}^+$ -BDT, CT/PVA, CT/TiO <sub>2</sub> , CMCT-benzaldehyde with or without starch		Steel, galvanized steel, MS	NaCl, HCl	Improved corrosion resistance
CT/CE and CT/La, CT/PVA, CT/BG, CT/CE		AZ91D magnesium, Mg WE43 alloy, Mg-1Ca	NaCl, DMEM, Kokubo's SBF	Showed corrosion inhibition
CT/GTFE/MBT, CT/MBT, CT/GTFE		2024-T3 aluminum alloy	NaCl	Improved corrosion protection
Cinn-CT, TCHECT and HECT, CT-3NiSA-S-MBT and CT-3NiSA-A-MBT	Mixing with corrosive media	Copper	HCl, HAc, $\text{Na}_2\text{SO}_4$ , NaOH, NaCl	Good corrosion inhibitors
CT/ATT, CMCT/ISP, CT/TC, CT/PASP, CT/TP, BHC and PHC, CT/SAH, polyCMCT-g-polyMVI, CT/CeO <sub>2</sub> , CMHPCT, CT-PEG, CT/AMT, CT-g-PEG and CT-g-PEG/AgNPs, CT/GA, CT/TU, VHCT, SL/CT, CT/SDBS, CT-g-Glu, CT/GTA, CT/GTA/DEAM, CTPTA and CTPTA-OA, CT/SAH, GTMACCT, CT/TS and CT/TC, CT/AgNPs, CMCT-g-PVI, CT/Co and CT/SnS <sub>2</sub> , CT-HQ, CT/SAH, CT/SAH/PANI/APS, CT/EDC/ $\text{Na}_2\text{EDTA}$ , CT/aldehyde, CMCT/AA, $\beta$ -CD-CT, CT/PNI, SCT, OFC, Pip-CT, CT/V, CT/AgNPs, TCHECT and HECT, CT-PEG, CMCT/AA, CT/AcSCN, CT/AgNO <sub>3</sub> , NCC and NHGZ		AISI 304 stainless steel, carbon steel 1020, A3 carbon steel, steel, P110 steel, J55 steel, APM on X70 steel, API 5L X70 steel, Q235 MS, MS, carbon steel, 5 L X70 steel, X80 pipeline steel, steel, API X70 steel, 304 steel	NaCl, $\text{CO}_2$ -saturated Mixture of NaCl, NaCl, $\text{CaCl}_2$ , $\text{MgCl}_2 \cdot 6\text{H}_2\text{O}$ , $\text{NaHCO}_3$ , and $\text{Na}_2\text{SO}_4$ , acidified NaCl, HCl, HAc, sulphamic acid, $\text{H}_2\text{SO}_4$ , Industrial water, municipal wastewater	Improved corrosion inhibition efficiency
CT-PA/TiO <sub>2</sub>		C3003 aluminum alloy	NaCl	Improved corrosion protection
A mixture of CT and other compounds	Mixing with corrosive media	Carbon steel, MS	HCl	Performed as an effective anticorrosive materials
CT with KI		Iron	$\text{H}_2\text{SO}_4$ , sulphamic acid	Increased corrosion protection ability
CT standalone	Coating	Zn	$\text{Na}_2\text{SO}_4$ , a mixture of $\text{Na}_2\text{SO}_4$ and $(\text{Fe}(\text{CN})_4)^{2-}$ + $(\text{Fe}(\text{CN})_6)^{3-}$	Good corrosion inhibitors
CT NPs		316L SS alloy	Hank's solution	Improved corrosion protection
CT		Aluminium 2024 alloy	NaCl	Showed corrosion inhibition
CT		Titanium grade 4	SBF	Improved corrosion inhibition efficiency
CT, CMCT		Copper	NaCl, HCl, sulphide polluted synthetic water	Increased corrosion protection ability
CT, CT NPs, CMCT	Mixing with corrosive media	MS, low carbon (X60 grade) steel, low carbon (API 5L X60 grade) steel, carbon steel, ST37 MS, austenitic stainless steel AISI 316, low carbon steel (Q235), St37-2	NaCl, HCl, HCl in addition of $\text{CH}_3\text{COOH}$ , $\text{H}_2\text{SO}_4$	Performed as an effective anticorrosive materials
CT		AZ31 Mg alloy	NaCl	Showed corrosion inhibition
CT		Aluminium alloy, aluminium (AA1005)	NaCl, $\text{H}_2\text{SO}_4$	Increased corrosion protection ability
CT		Iron	HCl	Improved corrosion protection

was mixed with hydrazinolysed epoxy-N-phthaloylchitosan (ECT) to form a TCHECT composite [50]. Other studies involved synthesizing CTFTC and CTFTS composites using CT, TC, and thiosemicarbazide (TS) [51]. The authors separately added TS and CT to CT dissolved in  $\text{CH}_3\text{COOH}$ , followed by HCHO addition, neutralization, precipitation, washing, and drying to obtain the composites. The CTFTC composite was synthesized using similar methods.

Similarly, Mouaden et al. [52] synthesized CT/TC composites using analogous approaches, while Chauhan et al. [53] produced CT/TS and CT/TC composites, closely following all steps but washing only with distilled water.

**Fig. 3** **a** Synthesis scheme of CH-HQ [55] and **b** Synthesis of Cht-PEG [53]



Additionally, TC was refluxed in a  $\text{CH}_3\text{COOH}$  solution to extract aminotriazolethiol (ATT), which was then mixed with CT dissolved in  $\text{CH}_3\text{COOH}$  to produce the CT/ATT nanocomposite [54].

CT and a 5-chloromethyl-8-hydroxyquinoline derivative (HQ), derived from 8-hydroxyquinoline (8-HQ), were utilized to prepare a CT-HQ corrosion inhibitor via a condensation reaction (Fig. 3a) [55]. In another study, CT was dissolved in dimethylformamide and acetic acid ( $\text{CH}_3\text{COOH}$ ) and then mixed with acetyl thiocyanate (AcSCN), obtained from the acetylation of dry ammonium thiocyanate ( $\text{NH}_4\text{SCN}$ ), followed by washing and drying

to produce a CT/AcSCN composite for use as a corrosion inhibitor [56]. Additionally, a CT/aldehyde-based composite was synthesized for corrosion inhibition [57]. This involved adding various aldehydes—such as chlorobenzaldehyde ( $C_7H_5ClO$ ), anisaldehyde ( $C_8H_8O_2$ ), butyraldehyde ( $CH_3(CH_2)_2CHO$ ), and octanaldehyde ( $CH_3(CH_2)_6CHO$ )—to CT dissolved in a  $CH_3COOH$  solution, followed by the addition of sodium borohydride ( $NaBH_4$ ), precipitation, and washing to obtain the composite.

CT was also modified prior to synthesizing the corrosion inhibitor composite. Eduok et al. [58] developed a poly(N-vinyl imidazole) grafted carboxymethyl chitosan composite (CMCT-g-PVI) as a corrosion inhibitor. They synthesized CMCT by reacting CT with chloroacetic acid in an alkaline medium, then dissolving it in water, purging with  $N_2$  gas, adding vinyl imidazole monomer and potassium persulfate, and finally washing and drying to yield CMCT-g-PVI. In a subsequent study, the same authors synthesized polyCMCT-g-polyMVI using CMCT and poly(2-methyl-1-vinylimidazole) (polyMVI) through a similar process [59]. To produce CMCT-benzaldehyde, CMCT dissolved in water was reacted with benzaldehyde in ethanol (1:1), followed by precipitation and washing [60]. Alsabagh et al. [57] created a CMCT/aldehyde-based composite using the same method as the CT/aldehyde-based composite and also prepared thio-CMCT products by extracting a filtrate from the reaction of acetonitrile,  $NH_4SCN$ , and octyl chloride, which was then added to CMCT, washed, and dried.

Furthermore, acetate-modified amylose (AA) was mixed with CMCT dissolved in chloric acid and CMCT dissolved in sulfate to prepare a CMCT/AA-based composite solution [61]. In another study, CMCT was incorporated into an isopropanol (ISP) solution to obtain a CMCT/ISP composite solution [62]. Additionally, CMCT and sodium dodecylbenzenesulfonate were dissolved in distilled water, followed by the addition of  $NaOH$ , allyl bromide, and washing to produce A-CMCT. For synthesizing  $\beta$ -CD-CT, A-CMCT and allylcyclodextrin (A- $\beta$ -CD) were dissolved in distilled water, neutralized, purged with  $N_2$ , and then initiators ( $(NH_4)_2S_2O_8$  and  $NaHSO_3^-$ ) were added, followed by washing and drying [63].

Previous studies have explored the development of corrosion inhibitors from ethanolic and CT solutions. For instance, an ethanolic solution of cinnamaldehyde (Cinn) was combined with CT dissolved in  $CH_3COOH$ , followed by microwave irradiation, precipitation, washing, and drying to yield the Cinn-CT Schiff base. Researchers also created a Cinn-CT Schiff base with slight modifications, using continuous reflux during microwave irradiation, followed by cooling, treatment with  $NaOH$ , and washing. Similarly, an ethanolic solution of 4-pyridinecarboxaldehyde (PA) was mixed with CT in  $CH_3COOH$ , stirred,

refluxed, cooled, centrifuged, washed, and dried to produce the CT-PA product. This product was then combined with  $TiO_2$  nanoparticles through ultrasonication and stirring, washed with ethanol and deionized water, and dried to form the CT-PA/ $TiO_2$  composite [64]. An ethanolic solution of piperonal (Pip) was also added to CT in  $CH_3COOH$ , followed by stirring and microwave irradiation. The mixture underwent reflux, cooling, precipitation in  $NaOH$  solution, washing, and drying to yield the Pip-CT Schiff base. Additionally, an ethanolic solution of 4-amino-5-methyl-1,2,4-triazole-3-thiol (AMT) was introduced to CT in  $CH_3COOH$ , stirred, and then treated with HCHO before refluxing. The resulting mixture was neutralized, filtered, and washed to obtain the CT/AMT composite. In another study, tetra butyl titanate, acetylacetone, and ethanol were mixed with CT in  $CH_3COOH$ , resulting in a CT/ $TiO_2$ -based composite solution [65]. Rbaa et al. [66] combined deacetylated CT in  $CH_3COOH$  with 1,5-anhydro-1,2-O-isopropylidene-D-glucofuranose (D-Glu) and absolute ethanol to develop the CT-g-Glu corrosion inhibitor. Additionally, ethanol was added to a mixture of CT in  $CH_3COOH$  and bioactive glass (BG) solution, which was then ultrasonicated for homogenization, resulting in a CT/BG solution [67]. A mixture of CT in methanol and vanillin (4-hydroxy-3-methoxy benzaldehyde, Van) dissolved in methanol was heated, stirred, and filtered to produce the VCT Schiff base. This product was then mixed with isopropanol and 3-chloro-2-hydroxypropyltrimethylammonium chloride (CHPTA), heated, and refluxed to obtain the CT-based N-Vanillyl-O-20-hydroxypropyltrimethylammonium chloride (VHCT) [68]. In another study, solubilized Vanillin in ethanol was added to CT in  $CH_3COOH$ , followed by irradiation, precipitation, washing, and drying to yield the CT/V composite product [69]. Finally, purified CT in  $CH_3COOH$  was mixed with polyvinyl alcohol (PVA) in water, sonicated, and dried to form a CT/PVA composite [70]. The CT/PVA composite was prepared using different methods in another study [71]. In this study, the authors first dissolved PVA in water by heating it, then mixed it with a similar CT solution and stirred the mixture at room temperature. Salicylaldehyde (SAH) dissolved in ethanol was then added to the CT dissolved in a  $CH_3COOH$  solution. The mixture underwent refluxing, filtering, washing, and drying to create a CT/SAH solution [72]. Similarly, a CT/SAH solution was prepared by precipitating it with acetone and subsequently washing it [73–75]. In another approach, Chen et al. [76] combined SAH with CT dissolved in ethanol, allowing the mixture to sit overnight. Afterward,  $CH_3COOH$  was added, and the mixture was refluxed, washed, and dried to yield the CT/SAH composite. Additionally, a mixture of CT and SAH was refluxed and cooled before adding polyaniline (PANI) and ammonium persulfate (APS). The resulting mixture was then washed

and dried to produce the CT/SAH/PANI/APS composite [77]. In a separate study, PANI dissolved in an  $\text{NH}_2\text{SO}_3\text{H}$  solution was added to CT dissolved in  $\text{CH}_3\text{COOH}$ . Following this, a solution of ammonium persulfate ( $(\text{NH}_4)_2\text{S}_2\text{O}_8$ ) dissolved in  $\text{CH}_3\text{COOH}$  was introduced. After the reaction completed, the mixture was filtered, washed, and dried to obtain the CT/PNI composite [78]. Furthermore, Jessima et al. [79] prepared a CT/EDC/ $\text{Na}_2\text{EDTA}$  product by adding an ethanolic solution of 1-Ethyl-3-(3-dimethylaminopropyl) carbodiimide (EDC) and disodium ethylenediaminetetraacetate ( $\text{Na}_2\text{EDTA}$ ) to dissolved CT. Similarly, a mixture of EDC and sodium lauryl sulfate (SL) was added to purified CT dissolved in HCl, followed by precipitation, washing, and drying to yield the SL/CT composite [80]. Li et al. [81] added glycidyl trimethyl ammonium chloride (GTA) to CT dissolved in water, followed by refluxing, precipitating, washing, and drying to obtain the CT/GTA composite. They further dissolved the CT/GTA in a  $\text{CH}_3\text{COOH}$  solution, added ethanol, and then introduced 4-Diethylaminobenzaldehyde (DEAM). The mixture was purified through similar steps to produce the CT/GTA/DEAM composite [81].

Lignosulfonate (LS) was dissolved in water and added to CT dissolved in acetic acid ( $\text{CH}_3\text{COOH}$ ), and the mixture was stirred. A cross-linking agent, formaldehyde (HCHO) combined with sulfuric acid ( $\text{H}_2\text{SO}_4$ ), was then mixed into the solution. The resulting mixture was centrifuged and washed to produce the CT/LS composite [82]. In a separate process to prepare sulfonated chitosan (SCT), 1,3-propanesultone was introduced to CT in acetic acid under heating. After the reaction, the mixture was cooled, precipitated, rinsed, and dried [83]. Additionally, Jia et al. [84] incorporated cerium nitrate hexahydrate ( $\text{Ce}(\text{NO}_3)_3 \cdot 6\text{H}_2\text{O}$ , CE) into CT dissolved in acetic acid, followed by ultrasonication to create a CT/CE composite solution. In another study, CT/La and CT/CE composites were prepared by combining lanthanum nitrate hexahydrate ( $\text{La}(\text{NO}_3)_3 \cdot 6\text{H}_2\text{O}$ , La) or  $\text{Ce}(\text{NO}_3)_3 \cdot 6\text{H}_2\text{O}$  with gelatin and CT, and then adjusting the pH [85].

An acidic solution was utilized to prepare CT-based corrosion inhibitors. El-Mahdy et al. [86] began by mixing CT with dissolved p-toluene sulfonic acid monohydrate (PTSA) in water. This mixture was then heated, mixed with acetone, washed, and dried to produce the CT-p-toluene sulfonate salt CTPTA composite. Next, oleic acid (OA) dissolved in methanol was added to the CTPTA solution in water, followed by precipitation, washing, and drying to yield the CTPTA-OA composite. In another study,  $(\text{NH}_4)_2\text{S}_2\text{O}_8$  was introduced to a mixture of CT in acetic acid ( $\text{CH}_3\text{COOH}$ ) and acrylic acid, resulting in the extraction of N-carboxylated chitosan (NCC) after the reaction was complete. NCC was then mixed with 2-hydroxyphosphonocarboxylic acid (HPAA), gluconic acid sodium (GA), and  $\text{ZnSO}_4$  to

synthesize the NHGZ composite [87]. Additionally, CT dissolved in a heptanoic acid solution was mixed with a dispersion of homoionic sodium beidellite ( $\text{Na}^+\text{-BDT}$ ), followed by washing and air-drying to obtain the CT/ $\text{Na}^+\text{-BDT}$  composite [33]. For the synthesis of a polyaspartic acid (PASP) and CT composite (CT/PASP), a PASP solution was added to CT dissolved in a  $\text{CH}_3\text{COOH}/\text{HCl}$  solution, followed by heating, filtering, and drying to create the CT/PASP composite [88, 89]. Sangeetha et al. [90] synthesized O-fumaryl-chitosan (OFC) for use as a corrosion inhibitor by adding fumaric acid to CT in a water suspension, followed by the addition of  $\text{H}_2\text{SO}_4$ . The mixture was stirred while heated, cooled, treated with  $\text{NaHCO}_3$ , extracted with ethanol using Soxhlet, and dried. Furthermore, hydroxypropyl chitosan (HPCT) was dissolved in water and alkalized before chloroacetic acid (CA) was added and refluxed. Subsequently,  $\text{CH}_3\text{COOH}$  was introduced, leading to precipitation, washing, and drying to produce carboxymethyl hydroxypropyl chitosan (CMHPCT) [91]. In a separate study, tryptophan (TP) was added to the CT solution, followed by the addition of  $\text{H}_2\text{SO}_4$ , resulting in precipitation, washing, and drying to obtain the CT/TP composite [92].

CT and slat-based corrosion inhibitors were also prepared. The researchers developed two types of quaternary ammonium salts: an N-benzyl CT oligosaccharide quaternary ammonium salt (BHC) and a CT oligosaccharide quaternary ammonium salt (PHC) for corrosion protection [36, 38]. To produce the N-(2-hydroxy) propyl-3-trimethyl ammonium CT oligosaccharide chloride (HTCT), the authors mixed CT oligosaccharide with glycidyl trimethyl ammonium chloride (GTMAC), followed by refluxing, precipitating, drying, dissolving in water, and lyophilizing. The lyophilized HTCT product was then reacted with benzaldehyde and propionaldehyde to yield BHC and PHC, respectively. In another study, GTMAC was added to the quaternary amine salt of CT dissolved in water. The mixture was then heated, precipitated, filtered, and dried to obtain the GTMACCT composite [93]. Additionally, CT quaternary ammonium salt was directly mixed with corrosive media [94], and hydroxyapatite (HA) was mixed with CT to prepare an HA/CT composite [95].

Research on polyethylene glycol (PEG) and CT-based corrosion inhibitors was conducted again. PEG was added to CT dissolved in a formic acid solution, followed by the addition of formaldehyde (HCHO). This mixture was then filtered, washed, and dried to produce the CT-PEG composite (Fig. 3b) [53]. In a separate study, CT-PEG was prepared by adding PEG aldehyde (mPEG-CHO) to CT dissolved in  $\text{CH}_3\text{COOH}$ . Sodium carbonate ( $\text{Na}_2\text{CO}_3$ ) and sodium borohydride ( $\text{NaBH}_4$ ) were then added, and the mixture was combined with a saturated solution of ammonium sulfate to precipitate the product. This precipitate was freeze-dried,

washed, and dried to yield CT-g-PEG. To create CT-g-PEG/AgNPs, silver nanoparticles (AgNPs) were mixed with the CT-g-PEG solution [96].

Glucosyloxyethyl acrylate (GA) dissolved in water was added to CT dissolved in  $\text{CH}_3\text{COOH}$ . After stirring, a sodium bicarbonate ( $\text{NaHCO}_3$ ) solution was introduced. The resulting mixture was poured into acetone, washed, filtered, sparged with nitrogen ( $\text{N}_2$ ), and dried to obtain the CT/GA composite [97]. In another study, CT was added to epichlorohydrin dissolved in acetone, followed by the addition of thiourea (TU) and stirring. The mixture was evaporated and precipitated in ethanol, then filtered, washed with ethanol, and dried to yield the CT/TU composite [98]. Additionally, CT was dissolved in  $\text{CH}_3\text{COOH}$ , stirred, and refluxed. The mixture was precipitated in acetone and rinsed with ethanol. Sodium dodecyl benzenesulfonate (SDBS), sodium hydroxide ( $\text{NaOH}$ ), and distilled water were then mixed with the CT solution. After placing the mixture in an ice-water bath, benzyl bromide was added, and stirring continued. The final product was filtered in ethanol to obtain the CT/SDBS composite [99]. Carbon dots (CDs) are increasingly popular in catalysis, sensors, and the optronics industry due to their high stability, good conductivity, low toxicity, and environmental friendliness. Additionally, they can serve as corrosion inhibitors. CDs can be produced from CT by dissolving it in a 1:1 mixture of  $\text{CH}_3\text{COOH}$  and water, followed by hydrothermal liquefaction [100]. Previous studies have shown that CT-based composites can be prepared as corrosion inhibitors through straightforward methods. For instance, a CT/MBT-based corrosion inhibitor was prepared by mixing mercaptobenzothiazole (MBT) with CT dissolved in  $\text{CH}_3\text{COOH}$  solution [34]. Carneiro et al. [101] prepared a CT/MBT composite using a similar method but added ethanol to enhance MBT solubility [101]. Similarly, CT solutions were mixed with cobalt (Co) and tin sulfide ( $\text{SnS}_2$ ) solutions to produce CT-Co and CT-SS composites, respectively [102]. Furthermore, glycidyl 2,2,3,3-tetrafluoropropyl ether (GTFE) was added to CT dissolved in  $\text{CH}_3\text{COOH}$  solution, followed by precipitation, washing, and drying to prepare the CT/GTFE composite [103, 104].

### 3.2 Combination with Other Compounds

In various studies, a combination of CT and other compounds has been utilized as corrosion inhibitors. Yavari et al. [105] combined CT with potassium iodide (KI) and hydrochloric acid (HCl), followed by filtering, washing, and drying. Similarly, CT and KI were used together as corrosion inhibitors in research by Gupta et al. [106] and Solomon et al. [107]. Additionally, CT was combined with  $(\text{NH}_4^+)_2\text{MoO}_4$ ,  $\text{ZnSO}_4$ , and  $\text{Na}_2\text{CrO}_4$  as corrosion inhibitors by Li et al. [108].

### 3.3 Chitosan Standalone

Researchers employed CT directly in corrosive media, while some prepared it beforehand. Zhang et al. [99] dissolved CT in  $\text{CH}_3\text{COOH}$ , then stirred, refluxed, precipitated it in acetone, and rinsed with ethanol before adding it to the corrosive media. Similarly, Szőke et al. [31] dissolved CT in  $\text{CH}_3\text{COOH}$  overnight, followed by centrifugation. In another study, Szőke et al. [109] also centrifuged dissolved CT in  $\text{CH}_3\text{COOH}$ , but did not specify the mixing time. De Sousa et al. [110] reported dissolving CT in  $\text{CH}_3\text{COOH}$  without detailing the conditions used. Additionally, Zhe ludkevich et al. [32] dissolved CT in  $\text{CH}_3\text{COOH}$ , filtered and degassed it, and then dissolved it in ethanol to prepare the solution. CT nanoparticles (CT NPs) were also prepared prior to their application in corrosive media. In this instance, sodium tripolyphosphate was added to the dissolved CT in  $\text{CH}_3\text{COOH}$  after stirring and filtration, followed by stirring and centrifugation to produce the CT NPs [30]. Other researchers also utilized CT NPs as a corrosion inhibitor [111]. CMCT was similarly prepared before being used as a corrosion inhibitor [112, 113].

## 4 Application and Corrosion Inhibition Performance

The type of metal and the corrosive environment both influence corrosion [114]. The effectiveness of CT-based corrosion inhibitors has been tested in various corrosive media through two main methods: coating metal surfaces and mixing inhibitors with corrosive media. In the first method, metal surfaces are coated with CT-based corrosion inhibitors before being submerged in corrosive environments. In the second method, metal samples are placed in a mixture of corrosive media and CT-based corrosion inhibitors. Table 1 summarizes the types of CT-based corrosion inhibitors, their application methods, and the metal surfaces used. An overview of the application techniques for CT-based corrosion inhibitors is illustrated in Fig. 4.

### 4.1 Chitosan-Based Composites as Corrosion Inhibitor

#### 4.1.1 Coating

CT-based composites have been utilized as coating materials to protect various metal surfaces from corrosion. For instance, a polished and cleaned aluminum alloy 2024-T3 was coated with CT/MBT formulations using a multi-layer dip-coating process at a constant speed of  $18 \text{ cm/min}^{-1}$ . This process involved applying five layers, each dried in a stream

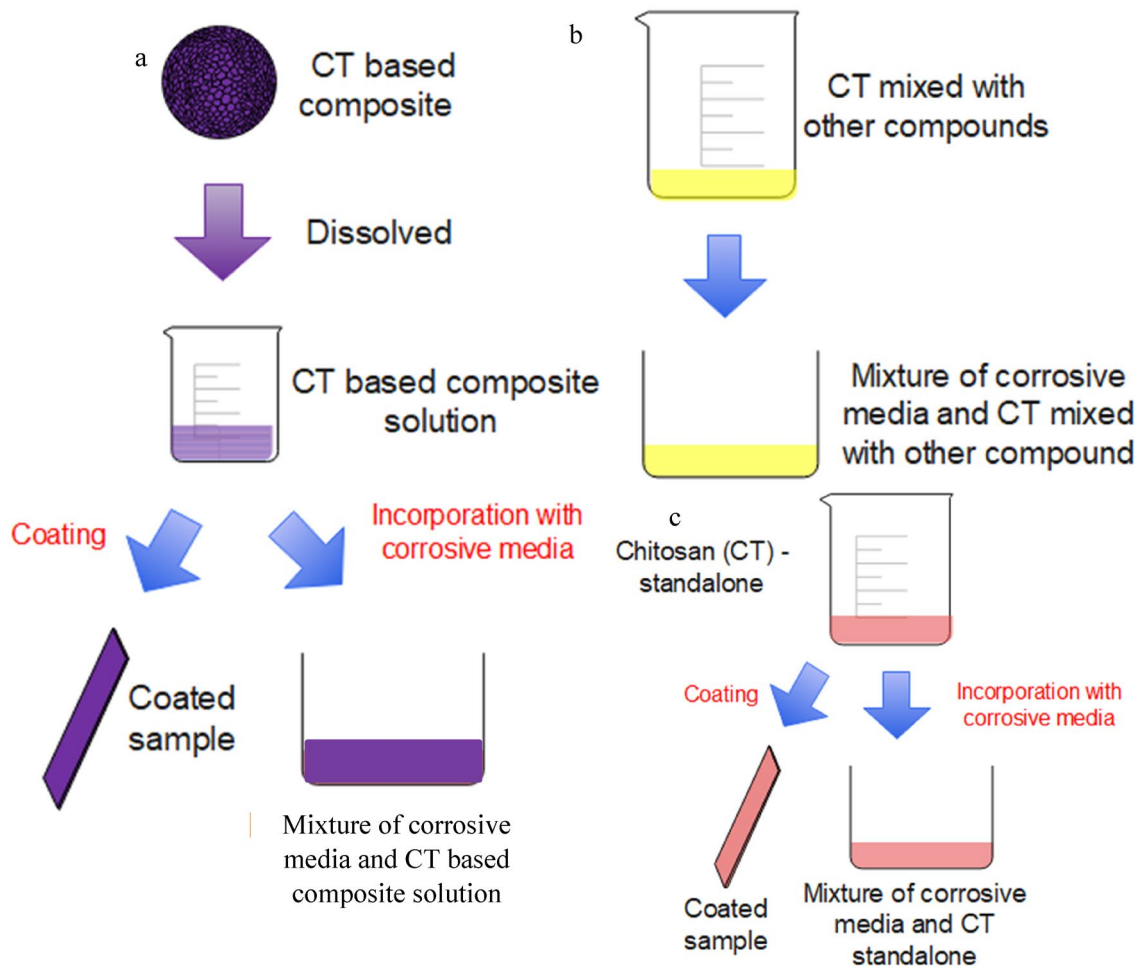


**Fig. 4** Application strategies of **a** CT-based composite, **b** CT mixed with other compounds, and **c** CT standalone as corrosion inhibitors

of hot air before the next layer was added [101]. In another study, Carneiro et al. [103] coated a similar aluminum alloy with a CT/GTFe composite solution using a dip-coater at a speed of  $9\text{ cm/min}^{-1}$ , applying ten layers. Additionally, the aluminum alloy was coated with a CT/GTFe/MBT solution following the same dip-coating technique. The coated samples were then immersed in glutaraldehyde (GA), poly(ethylene-alt-maleic anhydride) (PEMA), and poly(maleic anhydride-alt-1-octadecene) (POMA) dissolved in toluene, followed by washing and drying [104]. Similarly, a CT/PVA composite was applied to polished and cleaned AA8011 aluminum alloy at a coating speed of  $3\text{ cm min}^{-1}$ , achieving a thickness of  $5\pm 0.6\text{ }\mu\text{m}$  over four layers [71].

Steel samples were also treated with CT-based corrosion inhibitors to assess their effectiveness. Polished mild steel (MS) substrates were coated by repeatedly dipping them into a CT/AcSCN solution and then drying them under heat [56]. In another study, CMCT-benzaldehyde dissolved in distilled water, a  $\text{CH}_3\text{COOH}$ , and alcohol, with or without starch, was used to coat cleaned steel samples, which were

then immersed in the solution and dried [60]. A 30% CT/TiO<sub>2</sub> solution was applied to polished and cleaned MS samples via dip coating, with a coating speed of  $10\text{ m s}^{-1}$  and an immersion time of 10 s. The coated samples were left at room temperature overnight, and the process was repeated three times to achieve a uniform film thickness [65]. Additionally, a CT/Na<sup>+</sup>-BDT composite mixed with an alkyd resin emulsion was used to coat cleaned galvanized steel plates. The samples were immersed for 5 min, washed with distilled water and ethanol, and air-dried, resulting in a single layer with a thickness of 100  $\mu\text{m}$  [33]. A CT/PVA composite was also applied to MS samples, achieving a coating thickness of 50–60  $\mu\text{m}$  with a 30% solution concentration, and air-dried to create a protective film [70]. Zanca et al. [95] coated 304 stainless steel with an HA/CT composite using a galvanic deposition process. In another investigation, CD combined with nano Fe<sub>2</sub>O<sub>3</sub> was utilized to coat carbon steel BIS2062 samples to evaluate its corrosion efficiency (Fig. 5a, b) [100].

In addition to aluminium and steel, copper and magnesium were also coated with CT-based corrosion inhibitors.

For copper plates, CT/MBT/SiO<sub>2</sub>/GA was employed [47]. The authors began by priming the polished copper plates through immersion in an ethanolic solution of 11-mercaptopentadecanoic acid (MUA) under reflux conditions overnight. This was followed by rinsing with ethanol and drying. The copper plates were then coated layer-by-layer (LbL) using a dipping, drying, and washing process. MUA facilitated bonding with the copper plates through Cu–S covalent bonds and interactions between the dangling carboxylic and amine groups of CT. Similarly, MUA-modified polished and cleaned copper specimens were coated with a CT/MBT hydrogel using a dip-coater and were dried at room temperature [34]. Höhlinger et al. [67] coated polished and

cleaned Mg WE43 alloy with CT/BG using electrophoretic deposition (EPD) with a stainless steel anode (SS316L). In another study, CT/CE composite was used to coat polished and cleaned cubic Mg–1Ca plates [84], while CT/CE and CT/La were used for coating AZ91D magnesium alloys [85]. Additionally, a CT/Si-based product (SiCTBSEG and SiCTBSEG-cal) was utilized as a corrosion inhibitor [49].

The coated samples mentioned above were tested in various corrosive media with different concentrations. The investigations included CT/MBT [34] and CT/MBT/SiO<sub>2</sub>/GA [47] coated copper, CD, as well as nano Fe<sub>2</sub>O<sub>3</sub> coated steel BIS2062 [100], CT/PVA coated AA8011 aluminum alloy [71], and CT/CE and CT/La coated AZ91D magnesium [85], all immersed in a 3.5 wt.% NaCl solution. Additionally, CT/Na<sup>+</sup>-BDT coated galvanized steel was examined in a 3% NaCl solution [33], and CT/GTFe/MBT coated 2024-T3 aluminum alloy was tested in a 50 mM NaCl aqueous solution [104]. Other studies involved immersing CT/MBT [101] and CT/GTFe [103] coated 2024-T3 aluminum alloy in a 0.05 M NaCl solution to evaluate corrosion inhibition efficiency. Similarly, CT/PVA [70] and CT/TiO<sub>2</sub> [65] coated mild steel in a 0.1 N HCl solution, along with CMCT-benzaldehyde coated steel (with or without starch) in a 1.0 M HCl solution [60], were investigated for their corrosion inhibition efficiency. Furthermore, CT/BG coated Mg WE43 alloy was immersed in Dulbecco's modified eagle medium (DMEM), with or without fetal bovine serum (FBS), to measure corrosion inhibition efficiency [67]. In contrast, CT/CE coated Mg–1Ca plates were dipped in Kokubo's simulated body fluid (SBF) solution [84]. The corrosion inhibition efficiency was confirmed using electrochemical impedance spectroscopy (EIS) [33, 34, 47, 65, 70, 71, 85, 100, 101, 104], potentiodynamic polarization (PDP) [34, 65, 71], and weight loss studies [67, 84]. PDP studies demonstrated that both cathodic and anodic reactions were inhibited [34]. Furthermore, PDP results indicated that the corrosion current density was lower for the coated samples [85]. The studies also revealed that the corrosion inhibition was more effective for the coated steel samples containing higher concentrations of corrosion inhibitors [60]. Additionally, PDP experiments showed that increasing the inhibitor content led to a decrease in corrosion current, resulting in the formation of a protective layer that inhibited metal dissolution and hydrogen evolution. EIS results further demonstrated that charge transfer increased with higher concentrations of corrosion inhibitors, attributed to the formation of a protective coating on the metal surface [65]. The robustness of the coating was confirmed through various analyses, including field emission scanning electron microscopy (FESEM) [34, 70], scanning electron microscopy (SEM) [67, 71, 84, 85, 100, 101, 104], atomic force microscopy (AFM) [71, 100], energy dispersive

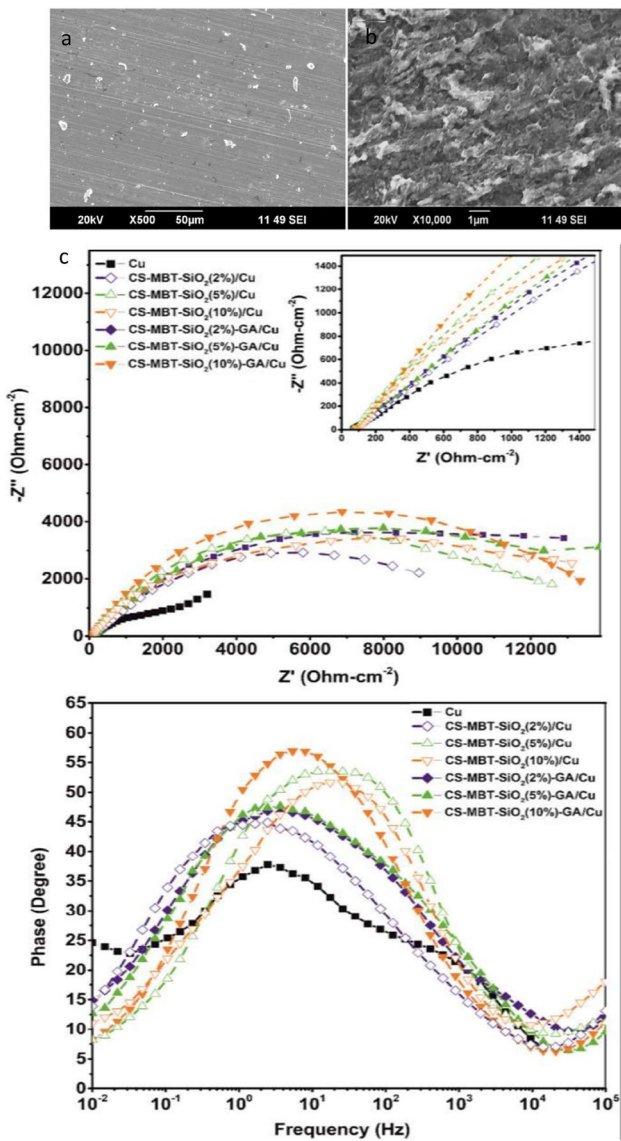


**Fig. 5** Scanning electron micrograph of CD coated over steel **a** untreated steel, **b** Nano-carbon dot treated steel to shows the layered structure of nano-CD over steel [100] and **c** Impedance spectra of crosslinked and non-crosslinked chitosan coating with MBT and SiO<sub>2</sub> additions [47]

spectrometry (EDS) [34, 84], X-ray diffraction spectroscopy (XRD) [65], Fourier transform infrared spectroscopy (FTIR) [70], thermogravimetric analysis (TGA) [70], and differential scanning calorimetry (DSC) [70].

The combination of MU with CT/MBT effectively protected copper from sulfide ions in NaCl solution [34]. CD can suppress oxidation and reduction reactions, thereby inhibiting corrosion [100]. The incorporation of MBT and SiO<sub>2</sub> improved the corrosion protection efficiency of CT-based coatings by reducing swelling [47, 101]. Crosslinked CT-based coatings demonstrated superior corrosion resistance compared to non-crosslinked versions, as confirmed by impedance measurements (Fig. 5c) [47]. The presence of heptanoate ions in CT/Na<sup>+</sup>-BDT, along with their continuous leaching as an inhibitor, further enhanced corrosion inhibition [33]. CT also acted as a carrier for Ce, facilitating better corrosion inhibition through the formation of Ce-NH<sub>2</sub> complexes [84]. Additionally, CMCT-benzaldehyde/starch was found to capture more H<sup>+</sup> ions, which increased corrosion inhibition [60]. The self-healing property of CT/GTFE provided enhanced corrosion protection [103]. Similarly, CT/PVA exhibited self-healing capabilities due to the interaction between PVA and Al ions, leading to improved corrosion protection. PVA, as an anodic inhibitor, further enhanced the corrosion inhibition of CT [71]. In another study, CT/BG coatings inhibited protein deposition, as confirmed by X-ray photoelectron spectroscopy (XPS), thereby increasing corrosion protection efficiency [67]. Enhanced hydrophobicity can also contribute to improved corrosion protection. Water contact angle measurements indicated that the CT-based composite-coated samples were hydrophobic [65]. The hydrophobicity of CT improved after grafting with PEMA and POMA, leading to more effective corrosion inhibition [104]. Conversely, the wettability of CT and the adhesion of the coating were enhanced by the presence of PVA, resulting in better corrosion inhibition [71].

#### 4.1.2 Incorporation with Corrosive Material

Researchers have mixed various concentrations of CT-based composites with different corrosive media in their studies. Metal samples were immersed in CT-based corrosion inhibitor-infused corrosive media to investigate corrosion inhibition efficiency. The performance of CT/ATT on AISI 304 stainless steel [54], CMCT/ISP on carbon steel 1020 [62], CT/TC on AISI 304 stainless steel [52], CT-PA/TiO<sub>2</sub> on C3003 aluminum alloy [64], CT/PASP on A3 carbon steel [88], and CT/TP on steel [92] was studied in a 3.5 wt.% NaCl solution. Additionally, the corrosion inhibition of BHC and PHC on P110 steel [36, 38] and CT/SAH on J55 steel [72] was investigated in CO<sub>2</sub>-saturated 3.5 wt.% NaCl solution. Another study examined the corrosion protection

of polyCMCT-g-polyMVI along with APM on X70 steel in corrosive media containing NaCl, CaCl<sub>2</sub>, MgCl<sub>2</sub>·6H<sub>2</sub>O, NaHCO<sub>3</sub>, and Na<sub>2</sub>SO<sub>4</sub> [59]. An acidified NaCl solution was used to assess the corrosion inhibition of CT/CeO<sub>2</sub> on API 5L X70 steel. Furthermore, the corrosion inhibition of nanocapsules (CT-3NiSA-S-MBT and CT-3NiSA-A-MBT) on copper in Na<sub>2</sub>SO<sub>4</sub> at pH 3, NaOH at pH 13, and NaCl at pH 6.5 solutions was explored [48].

Researchers have also utilized acidic media for corrosion protection analysis. The corrosion inhibition of CMHPCT on Q235 MS [91], CT-PEG on MS, CT/AMT on carbon steel, CT-g-PEG and CT-g-PEG/AgNPs on carbon steel [96], CT/GA on X70 steel [97], CT/TU on Q235 steel [98], VHCT on Q235 steel [68], SL/CT on MS [80], CT/SDBS on Q235 MS [99], CT-g-Glu on MS [66], CT/GTA and CT/GTA/DEAM on X80 pipeline steel [81], CTPTA and CTPTA-OA on steel [86], CT/SAH on Q235 steel [76], GTMACCT on MS [93], CT/TS and CT/TC on MS, CT/AgNPs on MS [46], CMCT-g-PVI on API X70 steel [58], CT/Co and CT/SnS<sub>2</sub> on MS [102], CT-HQ on MS [55], CT/SAH on MS [73–75], CT/SAH/PANI/APS on Q235 steel [77], Cinn-CT on copper, CT/EDC/Na2EDTA on MS samples [79], CT/aldehyde on API X65 steel [57], and CMCT/AA on MS [61] were studied in 1.0 M HCl solution. In contrast, the corrosion reduction of β-CD-CT on Q235 carbon steel and CT/PNI on Q235 steel [78] was measured in 0.5 M HCl solution [63], while the corrosion protection of SCT on carbon steel [83] and OFC on MS [90] was studied in 2 M HCl solution. Additionally, 15% HCl was used to analyze the corrosion protection of Pip-CT on carbon steel, CT/V on carbon steel [69], CT/AgNPs on St37 steel, and Cinn-CT Schiff base with or without KI on carbon steel. For CT-PEG [53] on MS, it was tested in 1 M sulphamic acid solution. Similarly, the corrosion inhibition of CMCT/AA on MS in 1 M H<sub>2</sub>SO<sub>4</sub> [61] and CT/AcSCN on MS in 0.5 M H<sub>2</sub>SO<sub>4</sub> solution [56] was investigated. Corrosion protection of TCHECT and HECT on 304 steel and copper sheet in 2% HAc (v/v) was also measured [50].

The performance of CT-based corrosion inhibitors was studied under real environmental conditions. For example, industrial water was used to evaluate the effectiveness of CT/AgNO<sub>3</sub> on mild steel [6]. Other research examined the corrosion inhibition of NCC and NHGZ composites on carbon steel in municipal wastewater [87]. Additionally, the CT/LS composite was tested in seawater [82].

The corrosion inhibition performance of CT-based composites in corrosive media was confirmed through various methods, including weight loss [36, 38, 48, 92], open circuit potential (OCP) [83], linear polarization resistance (LPR) [83], electrochemical impedance spectroscopy (EIS) [36, 38, 52, 54, 59, 72, 82], and potentiodynamic polarization (PDP) [52, 54, 59, 72]. EIS tests indicated that the formation

of a protective layer from the adsorption of inhibitors on the metal/solution interface improved corrosion protection, as evidenced by increased charge transfer resistance [36, 38, 52, 54, 59, 72, 82]. The presence of a protective film was confirmed by various analyses, including X-ray spectrometry (EDX) [36, 38, 52, 54], SEM [36, 38, 52, 59, 72, 82], atomic force microscopy (AFM) [36, 38, 72, 102], optical microscopy [59], stereo microscopy [68], XPS [72, 92], Fourier-transform infrared spectroscopy (FTIR) [73–76], and EDS [59]. The smooth surface observed also indicates the formation of a protective layer [114]. This film inhibits mass transfer, thereby providing corrosion protection [53].

Corrosion inhibition was found to increase with higher concentrations of inhibitors (Fig. 6a) [6], and PDP studies revealed that corrosion current densities decreased as inhibitor concentrations increased (Fig. 6b) [54]. PDP findings indicated that these inhibitors could act in various ways: as cathodic [36, 38, 72], anodic [88], mixed type [48, 66, 92], mixed type with cathodic predominance [97, 98], or mixed type dominated by anodic reactions [81]. Both EIS and PDP investigations demonstrated that corrosion inhibition improved as the concentration of inhibitors increased [52, 59, 72]. The adsorption of corrosion inhibitors on the steel surface reduces its wettability, resulting in enhanced corrosion protection [59].

Inhibitors were adsorbed through physical processes [6, 105], chemical processes [61], and a combination of both physical and chemical processes [52, 91, 98]. Additionally, inhibitors were adsorbed via physical, chemical, and retrodonation processes [81, 97]. Another study highlighted that inhibitors were primarily adsorbed through physical and chemical processes, with the chemical process being

particularly significant [66]. The synergistic effect of hydrogen bonds and physical and chemical absorption improved the corrosion inhibition efficiency of the CT-PA/TiO<sub>2</sub> composite [64]. Inhibitors that were either covalently linked or physically entrapped in nanocapsules were released in response to pH changes, thereby inhibiting corrosion [48]. In acidic conditions, CT-g-PEG and CT-g-PEG/AgNPs function as polycations due to protonation, allowing them to adsorb onto negatively charged metal surfaces, which inhibits corrosion [96]. The hydrophilic nature of CT/LS facilitates attachment to bacterial surfaces, damaging bacterial cell walls. Conversely, the formation of a CT/LS film on the metal surface prevents biofilm formation, contributing to corrosion inhibition [82]. Furthermore, the polar head and long hydrophobic alkyl chain of SL/CT enable efficient adsorption on metal surfaces and metal/solution interfaces [80].

#### 4.2 Mixed Chitosan with Other Compounds as Corrosion Inhibitors

CT-based corrosion inhibitors were added to corrosive media to evaluate their effectiveness. For instance, CT/KI was introduced to a 1 M sulphamic acid solution to assess its corrosion inhibition of mild steel [106]. Additionally, the corrosion inhibition of CT/KI on iron in H<sub>2</sub>SO<sub>4</sub> solution was measured [105]. In another study, CT was used as a corrosion inhibitor in combination with (NH<sub>4</sub>)<sub>2</sub>MoO<sub>4</sub>, ZnSO<sub>4</sub>, and Na<sub>2</sub>CrO<sub>4</sub> [108].

Moreover, the effectiveness of corrosion inhibition is affected by both the temperature of the corrosive media and the duration of immersion. For CT/KI, increasing the

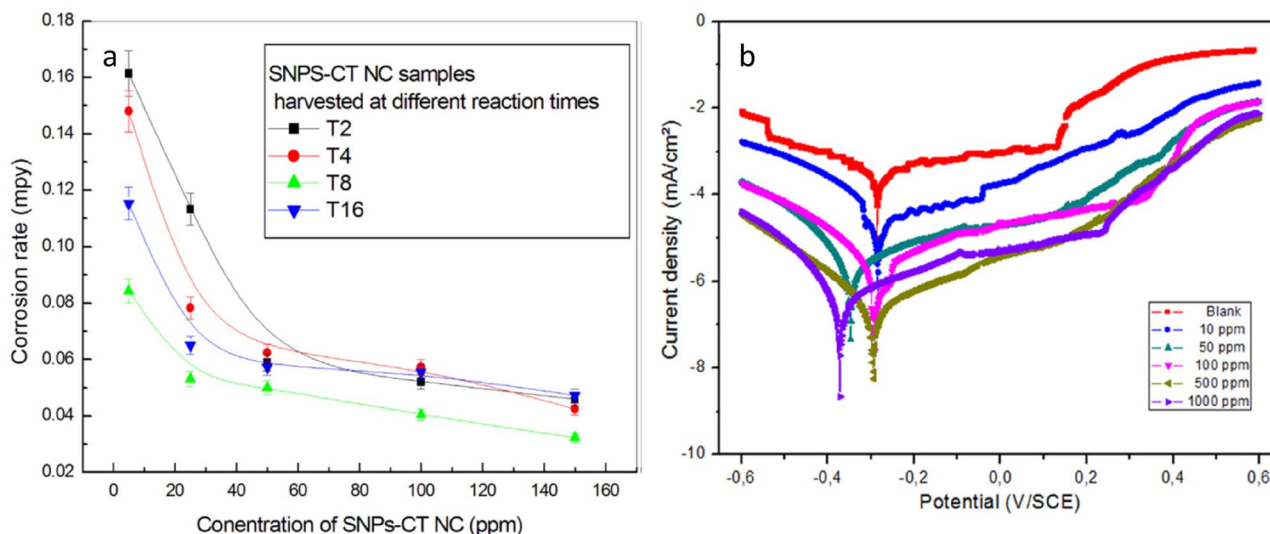


**Fig. 6** **a** The corrosion rate (along with the error bars) of mild steel in chilled water in the presence of different concentrations of nanocomposite samples [6] and **b** Potentiodynamic polarization curves of

stainless steel in 3.5% NaCl without and with CT/ATT at different concentrations [54]. Symbols refer to SNPs-CT NC=CT/AgNO<sub>3</sub> and T=time in h

temperature improved its corrosion protection capabilities. The dynamic electrochemical impedance spectroscopy (DEIS) study indicated that CT/KI exhibited greater inhibition efficiency with longer immersion times.

### 4.3 Chitosan Standalone as Corrosion Inhibitor

#### 4.3.1 Coating

Similar to CT-based composites, a standalone CT was utilized to coat metal surfaces to prevent corrosion. The CT was applied to zinc (Zn) plates through dip coating, maintaining a constant immersion and withdrawal speed of  $5\text{ cm min}^{-1}$  at  $25\text{ }^{\circ}\text{C}$ , followed by a drying process. Subsequently, 2-acetylaminio-5-mercaptop-1,3,4-thiadiazole (AcAMT) was impregnated into the CT-coated samples using a 1 mM aqueous solution of AcAMT, with a dip coating speed of  $1\text{ cm min}^{-1}$  for 15 min, and rinsing with distilled water [31]. In a similar approach, Szőke et al. [109] coated Zn plates with CT via dip coating at a speed of  $5\text{ cm min}^{-1}$ , then dried the samples. They also impregnated the coated samples with a 1 mM aqueous indigo carmine solution, using an immersion speed of  $1\text{ cm min}^{-1}$  for 15 min.

In addition to Zn, researchers also investigated aluminum, steel, and titanium. The CT and an ethanolic solution of CT were applied to aluminum 2024 alloy substrates in two dip-coating steps. The first step involved applying four layers of the ethanolic solution at a speed of  $9\text{ cm min}^{-1}$ , followed by a second step where ten layers of the CT solution were applied at  $18\text{ cm min}^{-1}$ . To create Ce-containing CT films,  $\text{Ce}(\text{NO}_3)_3$  was incorporated into the chitosan solution. Prior to coating, the metal was cleaned using alkaline and acid etching techniques, followed by washing [32]. In other studies, CT nanoparticles (NPs) were used to coat bare 316L stainless steel (SS) alloy [30]. The alloy was dipped in glutaraldehyde and dried, while steel was coated with a chitosan derivative (CD) [100]. A biomimetic method was employed to coat titanium substrates with CT [110]. This involved an alkaline treatment to create active sites for hydroxyapatite precipitation, followed by heat treatment, cooling, and immersion in simulated body fluid (SBF). The titanium was then immersed in  $\text{AgNO}_3$  and subsequently in a CT solution.

To assess the corrosion inhibition efficiency of CT, the coated samples were exposed to various corrosive media. The studies investigated the corrosion inhibition of CT-coated Zn with or without AcAMT in a  $\text{Na}_2\text{SO}_4$  solution (pH 5) [31], CT-coated Zn in  $\text{Na}_2\text{SO}_4$  and a mixture of  $\text{Na}_2\text{SO}_4$  with  $(\text{Fe}(\text{CN})_4)^{2-} + (\text{Fe}(\text{CN})_6)^{3-}$  solution [109], CT and ethanolic solution-coated aluminium 2024 alloy in 0.05 M  $\text{NaCl}$  [32], CT NPs coated 316L SS alloy in Hank's solution [30],

and CT-coated commercially pure titanium grade 4 in SBF [110].

The corrosion inhibition efficiency of CT-coated samples was analyzed using open circuit polarization (OCP) [110], electrochemical impedance spectroscopy (EIS) [30, 31, 109], and potentiodynamic polarization (PDP) studies [30, 109]. The presence of the coating layer was confirmed through scanning electron microscopy (SEM) [30, 109, 110], EDS [110], XRD [110], and energy-dispersive X-ray (EDX) studies [30]. The inhibitors were adsorbed via physical and chemical processes, with the chemical process being predominant [30]. PDP studies indicated that CT functions as a mixed-type inhibitor [109]. EIS studies demonstrated that CT-coated zinc samples impregnated with AcAMT exhibited higher corrosion resistance, as CT enhanced the accumulation of AcAMT on the zinc surface, leading to improved inhibition efficiency [31]. A complex interaction between the functional groups of CT macromolecules and cerium ions ( $\text{Ce}^{3+}$ ) facilitates the prolonged release of the active agent to inhibit corrosion. Self-healing capabilities were confirmed through a localized electrochemical study in micro-confined defects [32].

#### 4.3.2 Incorporation with Corrosive Material

CT was mixed directly with corrosive media in various studies, utilizing different concentrations of CT and corrosive agents. The corrosion inhibition effects of CT were examined on copper [115] and AZ31 magnesium alloy in a 3.5 wt.%  $\text{NaCl}$  solution. Similarly, a 3.65%  $\text{NaCl}$  solution was employed to assess the corrosion inhibition performance of CT on aluminum alloy [116] and CT nanoparticles on mild steel (MS) [111]. Additionally, the corrosion inhibition of CT on copper was measured in a 3%  $\text{NaCl}$  solution [117]. Other studies investigated the corrosion inhibition of CT on low-carbon (X60 grade) steel and the combined effects of CMCT and CT on low-carbon (API 5L X60 grade) steel in a  $\text{CO}_2$ -saturated 3.5 wt%  $\text{NaCl}$  solution, while a  $\text{FeCl}_3$  solution was used for CT on 2205 duplex stainless steel [118].

Various acidic media at different concentrations were also used to analyze corrosion inhibition efficiency. The corrosion inhibition effects of CMCT on steel [35], CT on copper [119], CT on iron [120], CT on carbon steel [121], and CMCT on MS [112] were measured in a 1 M  $\text{HCl}$  solution. In another study, the corrosion inhibition of CT on copper in a 0.5 M  $\text{HCl}$  solution was investigated [37]. Additionally, corrosion inhibition of CT on ST37 mild steel [122] and on austenitic stainless steel AISI 316 in a 0.1 M  $\text{HCl}$  solution was studied. A 0.1 M  $\text{HCl}$  solution combined with  $\text{CH}_3\text{COOH}$  was used to assess the corrosion inhibition efficiency of CT on MS. Furthermore, the corrosion inhibition of CT and CMCT on low carbon steel (Q235) in a

5% (v/v) HCl solution was examined [113]. The effects of CT on aluminum (AA1005) in a 1 M H<sub>2</sub>SO<sub>4</sub> solution [123] and on St37-2 in a 15% H<sub>2</sub>SO<sub>4</sub> solution were also evaluated. Mouaden et al. [124] studied the corrosion inhibition efficiency of CT on copper in a real environment using sulphide-polluted synthetic water.

The corrosion inhibition efficiency of CT was analyzed using weight loss [35, 111, 116, 117, 119], open circuit potential (OCP) [111, 116, 119, 122], electrochemical impedance spectroscopy (EIS) [115–117, 119], and PDP studies [111, 115–117, 119]. OCP and weight loss studies indicated that corrosion resistance improved with increasing inhibitor concentration [111, 116, 119]. EIS results showed that a protective film led to an increase in polarization resistance with concentration (Fig. 7a) [115–117, 121]. The formation of this protective film was confirmed through optical micrographs [115], SEM (Fig. 7b–d) [37, 117, 119], EDX [119], atomic force microscopy (AFM) [119, 122], FTIR [37], EDS [122], XPS [113], and XRD [113] analyses.

CT was adsorbed according to the Langmuir adsorption isotherm model [112, 123]. The CT inhibitor exhibited various types depending on the corrosive medium, including cathodic [117], anodic, mixed [35, 37, 111, 116, 121, 123], and mixed with a cathodic trend [112, 115, 119]. Additionally, the CT inhibitor was adsorbed through different processes in various corrosive media, primarily through physical and chemical processes, with the physical process being predominant [115]. The adsorption process was characterized as both physical and chemical with spontaneous characteristics [123]. Other studies suggested that the adsorption process was of a physical and chemical nature [35, 37, 119, 122]. Conversely, Razali et al. [112], Eddib et al. [125], and Mouaden et al. [124] concluded it was solely physical. However, other investigations indicated that the absorption process for CT inhibitors was both physical [116] and spontaneous [117], while some studies noted it was absorbed through physical, endothermic, and spontaneous processes [120, 121].

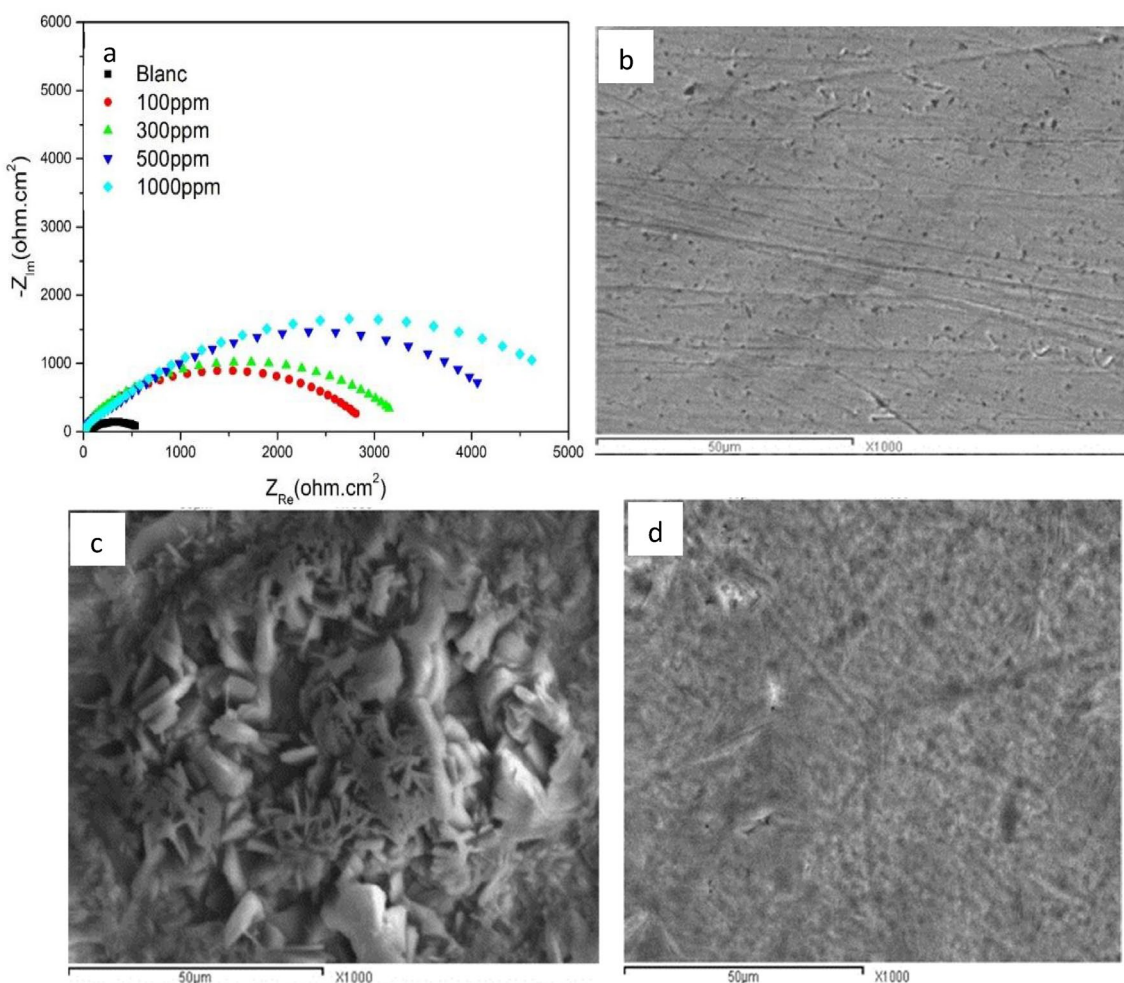


**Fig. 7** **a** Nyquist diagrams for copper in blank solution and with different concentrations of chitosan [115]; SEM micrographs of **b** freshly polished copper specimen, **c** the specimen immersed in 0.5 HCl solutions for 12 h at  $25 \pm 1$  °C without chitosan and **d** with  $8 \times 10^{-6}$  M chitosan [37]

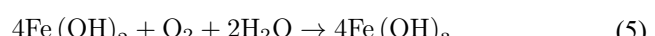
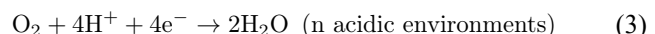
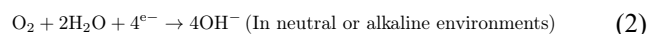
CT NPs inhibit corrosion by blocking the anodic and cathodic sites on steel and forming a thin film on the surface [111]. The highest negative charges from the heteroatoms N<sub>2</sub> and O<sub>2</sub> in CT are adsorbed onto the metal surface [37, 119]. The spontaneous adsorption of CT molecules on the copper surface can be explained by molecular dynamics simulations [119].

The corrosion resistance efficiency of CT is influenced by temperature and immersion time. Increasing temperatures tend to decrease corrosion inhibition efficiency [118–121]. However, at certain limits, higher temperatures can enhance corrosion resistance. Elevated temperatures increase the formation of H<sup>+</sup>, which in turn raises the corrosion rate [120]. Longer immersion times improve corrosion inhibition efficiency due to the increased thickness of the protective film resulting from stronger molecular adsorption. Nevertheless, Mouaden et al. [124] noted that this efficiency was not dependent on immersion time.

## 5 Mechanism of Corrosion and Inhibition by Chitosan-Based Corrosion Inhibitor

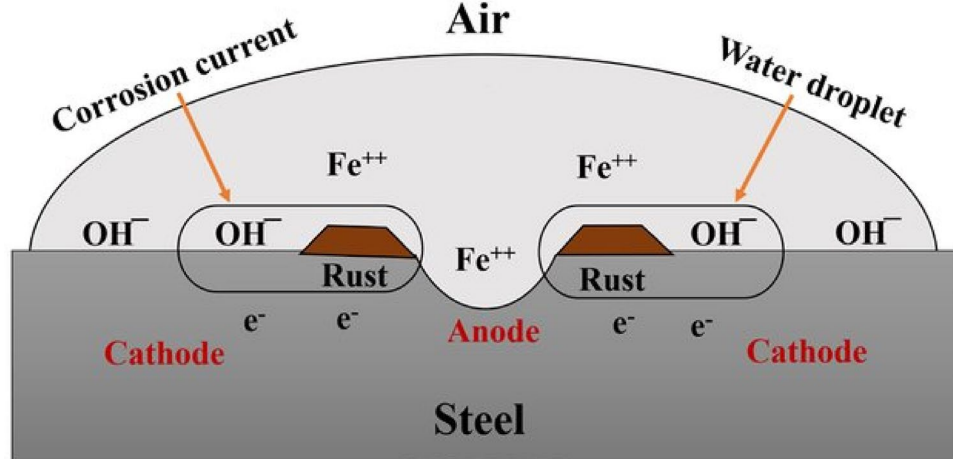
The corrosion mechanism of metals involves electrochemical reactions between the metal surface and its environment, often in the presence of water and oxygen. In an anodic reaction (oxidation), the metal loses electrons and forms positively charged metal ions; for example, iron transforms into iron ions (Fe<sup>2+</sup>) (Eq. 1). In the cathodic reaction (reduction), these released electrons reduce oxygen, typically in the presence of water, resulting in the formation of hydroxide ions (Eqs. 2 and 3) [126]. Rust formation is also part of this corrosion process. During rust formation, the metal ions (Fe<sup>2+</sup>) and hydroxide ions (OH<sup>-</sup>) react to form iron(II) hydroxide (Eq. 4), which can further oxidize to iron(III) hydroxide (Eq. 5) and ultimately lead to the formation of

hydrated iron oxides [127]. An example of a corrosion mechanism for steel is illustrated in Fig. 8.



The strong interaction between metals and organic inhibitors displaces water molecules from the metal surface [87]. The presence of functional groups significantly influences the corrosion inhibition process [129, 130]. Inhibitors deposit on anodic sites due to a donor–acceptor interaction between the electron pairs from the inhibitor molecules and the Fe<sup>2+</sup> ions on the metal surface. To prevent hydrogen evolution, the protonated form of the quaternary amine group, present in acidic media, is adsorbed onto the cathodic sites (Fig. 9a). Consequently, the corrosion inhibition of mild steel (MS) by GTMACCT occurs because of the electron pair on nitrogen and the positive charge of the quaternary ammonium group [93]. The electric double layer inhibits ion permeation, which in turn protects the metal from corrosion. Furthermore, the electron pairs from –C=N and –OH groups can adsorb onto the anodic sites of the metal surface that have empty d orbitals through chemical interaction. This results in the chemical adsorption of CMCT, forming coordination bonds between the active sites and the accessible d-orbitals of the MS surface, thus offering protection against corrosion (Fig. 9b) [62]. The benzene ring of salicylaldehyde contains  $\pi$  electrons that can share electrons with the MS atom to enhance interaction. Consequently, CT Schiff base undergoes chemical adsorption by forming

**Fig. 8** Corrosion mechanism of steel [128]



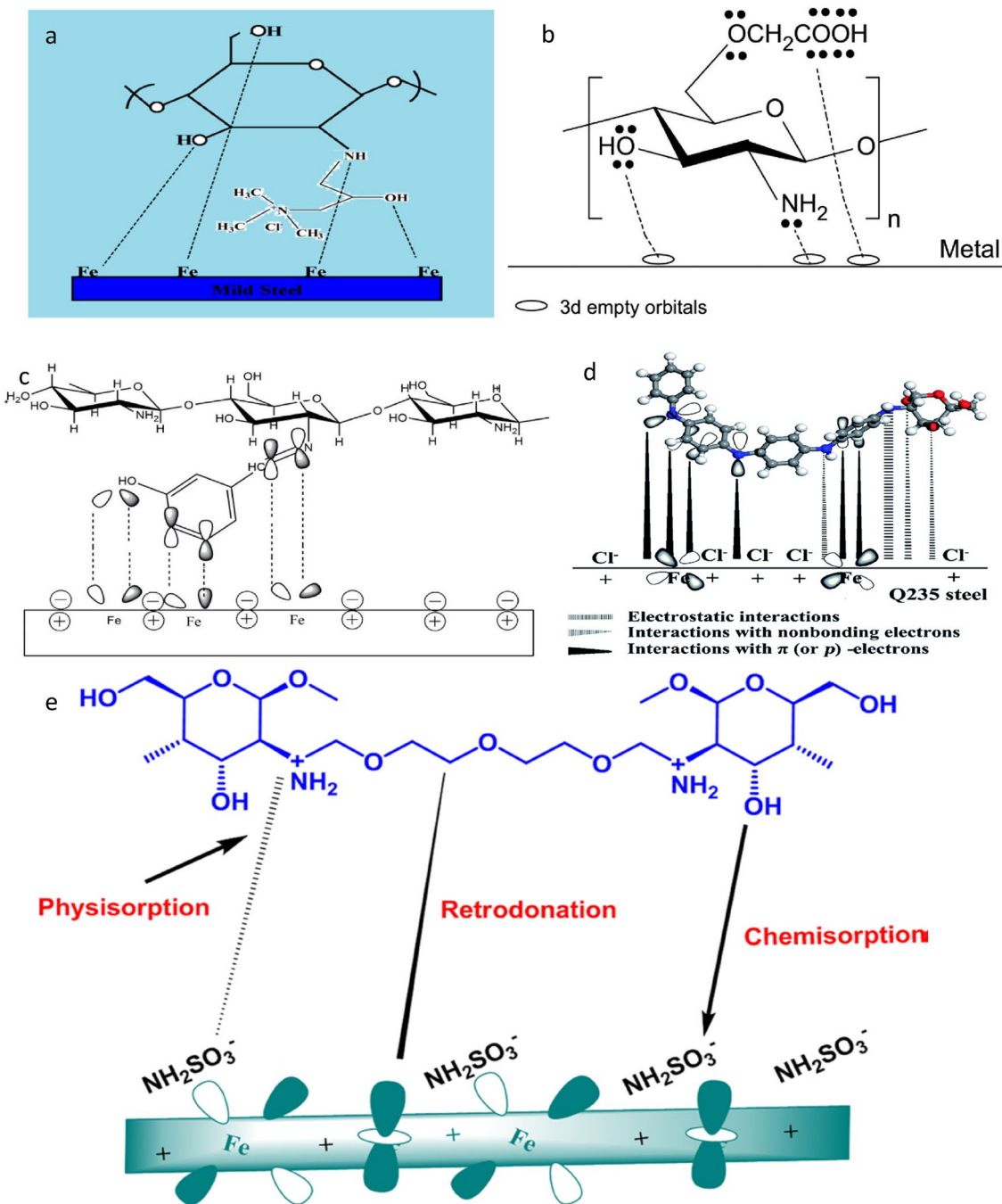


**Fig. 9** **a** Mechanism of corrosion inhibition [93], **b** Scheme of CMCT adsorption mechanism onto the metal surface [62]. **c** Schematic representation of plausible interaction of inhibitor with the metal surface

[73]; **d** A schematic diagram of the proposed inhibition mechanism of PANI/CTS on mild steel/0.5 M HCl interface [78] and **e** Schematic of the mechanism of adsorption of Cht-PEG on the mild steel surface [53]

coordination bonds between its active sites and the available d-orbitals of the MS surface, thereby inhibiting corrosion (Fig. 9c) [73–75]. The adsorption of PANI/CTS to the steel surface is facilitated by the electron-donating N<sub>2</sub>, O<sub>2</sub>, –C=N groups, and the aromatic ring of PANI/CTS. Corrosion is inhibited due to the synergistic interaction between the adsorbed chloride ions and PANI/CTS, the displacement

of water molecules from the steel surface, and the electron sharing between nitrogen/oxygen atoms and iron resulting from PANI/CTS's adsorption on the steel surface (Fig. 9d) [78]. Various theories have been established to explain the adsorption of inhibitors on the metal surface. A study utilizing density functional theory (DFT) demonstrated that the interaction between CT-HQ and the MS surface occurs

through a donor–acceptor mechanism [55]. In contrast, the Langmuir isotherm illustrates the physical and chemical adsorption of inhibitors. During the corrosion reaction, the metal surface becomes more negatively charged, causing the partially filled d-orbitals of the metal to be transformed into vacant  $\Pi$  antibonding orbitals through a retrodonation process (Fig. 9e). As a result, corrosion inhibitor molecules are adsorbed onto the metal surface [53].

The adsorption of these inhibitors reduces the number of active sites available on the steel surface [55]. Consequently, inhibitors can enhance the hydrophobic characteristics of metal surfaces. Measurements of water contact angles indicated that the addition of corrosion inhibitors increased hydrophobicity [81, 83]. For instance, the hydrophobic benzyl group present in CT/SDBS contributed to a higher electron density at active sites, thereby effectively covering the Q235 steel surface and improving performance [99]. Additionally, the presence of a longer hydrophobic segment in CT/aldehyde further enhanced inhibition efficiency [57]. Moreover, the modified anionic CT surfactant with a hydrophobic tail could produce monodisperse and stable AgNPs, leading to better corrosion protection [46]. Ultimately, these inhibitors reduce the anodic dissolution of MS, resulting in a decrease in the corrosion current.

## 6 Challenges and Future Outlook

Using CT as a corrosion inhibitor presents several challenges that may limit its effectiveness or applicability in different environments. Solubility is a major issue. CT is only soluble in acidic conditions (typically at pH below 6.5) [131], which can limit its use in neutral or alkaline environments. This restricts its direct application as a corrosion inhibitor in some industrial processes. The solubility of CT in water is low [132], which can make it difficult to prepare stable formulations for use in aqueous corrosion systems. The stability of CT in corrosive media is also a concern. It can degrade under harsh chemical conditions or at high temperatures, reducing its effectiveness as a long-term corrosion inhibitor [13]. The stability in various corrosive media is challenging as well. For example, maintaining the stability of CT-based corrosion inhibitors' coatings or films on metal surfaces can be challenging, especially in environments that involve fluctuating pH, temperature, or the presence of aggressive ions such as chlorides. Furthermore, the effectiveness of CT as a corrosion inhibitor can vary depending on the type of metal or alloy it is used with. It may work well on certain metals like steel, but be less effective on others, requiring further modification or use in combination with other inhibitors. The adhesion compatibility between CT and the metal surface is critical for forming a protective

barrier. Certain metal surfaces may require additional surface treatment for better CT adherence. Addressing these challenges often requires balancing the natural properties of chitosan with necessary chemical modifications or adjustments to suit specific applications. Therefore, the following actions should be considered:

- It is essential to improve the properties of CT, such as solubility and adhesion. This can be achieved through various chemical modifications or additives, and the effectiveness of these modifications should be clearly justified.
- Utilizing CT-based corrosion inhibitors in different corrosive environments, circumstances, and metals can help determine their overall effectiveness in inhibiting corrosion.

For all types of CT-based corrosion inhibitors, it is important to examine how temperature and time influence their ability to inhibit corrosion.

## 7 Conclusions

Chitosan (CT) can be used as a corrosion inhibitor to protect metal surfaces across various industries. To evaluate its effectiveness, CT-based composites, which are combinations of CT and active compounds, as well as pure CT, have been tested as coating materials and mixed with corrosive media. Their application in acidic, alkaline, and industrial environments has shown positive results in inhibiting corrosion. However, further research is needed to assess the effectiveness of a single CT-based inhibitor for different types of metals, considering the optimal conditions and varying corrosive environments.

**Author Contributions** Atanu Kumar Das: Conceptualization, Methodology, Literature review, Writing – original draft, Writing—Review & Editing, Visualization Md Nazrul Islam: Conceptualization, Writing—Review & Editing David A. Agar: Writing—Review & Editing, Roni Maryana: Writing—Review & Editing Magnus Rudolfsson: Writing—Review & Editing.

**Funding** Open access funding provided by RISE Research Institutes of Sweden. This research did not receive any specific grant from funding agencies in the public, commercial, or not-for-profit sectors.

**Data Availability** No datasets were generated or analysed during the current study.

## Declarations

**Conflict of interest** The authors declare no competing interests.

**Ethical Approval** None.

**Consent to Participate** None.

**Consent for Publication** None.

**Open Access** This article is licensed under a Creative Commons Attribution 4.0 International License, which permits use, sharing, adaptation, distribution and reproduction in any medium or format, as long as you give appropriate credit to the original author(s) and the source, provide a link to the Creative Commons licence, and indicate if changes were made. The images or other third party material in this article are included in the article's Creative Commons licence, unless indicated otherwise in a credit line to the material. If material is not included in the article's Creative Commons licence and your intended use is not permitted by statutory regulation or exceeds the permitted use, you will need to obtain permission directly from the copyright holder. To view a copy of this licence, visit <http://creativecommons.org/licenses/by/4.0/>.

## References

1. Montemor MF (2014) Functional and smart coatings for corrosion protection: a review of recent advances. *Surf Coat Technol* 258:17–37
2. Deyab MA (2013) Effect of halides ions on  $H_2$  production during aluminum corrosion in formic acid and using some inorganic inhibitors to control hydrogen evolution. *J Power Sources* 242:86–90
3. Deyab MA, Eddahaoui K, Essehli R, Rhadfi T, Benmokhtar S, Mele G (2016) Experimental evaluation of new inorganic phosphites as corrosion inhibitors for carbon steel in saline water from oil source wells. *Desalination* 383:38–45
4. Azani N, Haafiz MKM, Zahari A, Poinsignon S, Brosse N, Hussein MH (2020) Preparation and characterizations of oil palm fronds cellulose nanocrystal (OPF-CNC) as reinforcing filler in epoxy-Zn rich coating for mild steel corrosion protection. *Int J Biol Macromol* 153:385–398
5. Ashassi-Sorkhabi H, Kazempour A (2020) Chitosan, its derivatives and composites with superior potentials for the corrosion protection of steel alloys: a comprehensive review. *Carbohydr Polym*. <https://doi.org/10.1016/j.carbpol.2020.116110>
6. Fetouh HA, Hefnawy A, Attia AM, Ali E (2020) Facile and low-cost green synthesis of eco-friendly chitosan-silver nanocomposite as novel and promising corrosion inhibitor for mild steel in chilled water circuits. *J Mol Liq*. <https://doi.org/10.1016/j.molliq.2020.114355>
7. Espinoza-Acosta JL, Torres-Chavez PI, Ramirez-Wong B, Lopez-Saiz CM, Montano-Leyva B (2016) Antioxidant, antimicrobial, and antimutagenic properties of technical lignins and their applications. *BioResources* 11:5452–5481
8. Deyab MA, Eddahaoui K, Essehli R, Benmokhtar S, Rhadfi T, De Riccardis A, Mele G (2016) Influence of newly synthesized titanium phosphates on the corrosion protection properties of alkyd coating. *J Mol Liq* 216:699–703
9. Lyon SB, Bingham R, Mills DJ (2017) Advances in corrosion protection by organic coatings: what we know and what we would like to know. *Prog Org Coat* 102:2–7
10. Athawale VD, Nimbalkar RV (2011) Waterborne coatings based on renewable oil resources: an overview. *J Am Oil Chem Soc* 88:159–185
11. Elrebbi M, Ben Mabrouk A, Boufi S (2014) Synthesis and properties of hybrid alkyd-acrylic dispersions and their use in VOC-free waterborne coatings. *Prog Org Coat* 77:757–764
12. He YJ, Boluk Y, Pan JS, Ahniyaz A, Deltin T, Claesson PM (2019) Corrosion protective properties of cellulose nanocrystals reinforced waterborne acrylate-based composite coating. *Corros Sci* 155:186–194
13. Ravi Kumar MNV (2000) A review of chitin and chitosan applications. *React Funct Polym* 46:1–27
14. Carneiro J, Tedim J, Ferreira MGS (2015) Chitosan as a smart coating for corrosion protection of aluminum alloy 2024: a review. *Prog Org Coat* 89:348–356
15. Al Kiey SA, Hasanin MS, Heakal FE (2022) Green and sustainable chitosan-gum Arabic nanocomposites as efficient anticorrosive coatings for mild steel in saline media. *Sci Rep*. <https://doi.org/10.1038/s41598-022-17386-7>
16. Alotaibi WM, Al-Mhyawi SR, Albukhari SM (2022) Chitosan-clay nanocomposite as a green corrosion inhibitor for mild steel in hydrochloric acid solution. *Int J Electrochem Sci*. <https://doi.org/10.20964/2022.08.50>
17. Arwati IGA, Majlan EH, Alva S, Muhammad W (2022) Effect of chitosan on the corrosion inhibition for aluminium alloy in  $H_2SO_4$  medium. *Energies*. <https://doi.org/10.3390/en15228511>
18. Cui GD, Zhang QM, Zhao Q, Wang Z, Tang T, He X, Cui S, Li X, Liu YS (2022) Synthesis of branched chitosan derivatives for demulsification and steel anti-corrosion performances investigation. *Colloids Surf A-Physicochem Eng Asp*. <https://doi.org/10.1016/j.colsurfa.2022.130038>
19. Dalhatu SN, Modu KA, Mahmoud AA, Zango ZU, Umar AB, Usman F, Dennis JO, Alsadig A, Ibnaouf KH, Aldaghri OA (2023) L-arginine grafted chitosan as corrosion inhibitor for mild steel protection. *Polymers*. <https://doi.org/10.3390/polym15020398>
20. Fernandez-Solis C, Keil P, Erbe A (2023) Molybdate and phosphate cross-linked chitosan films for corrosion protection of hot-dip galvanized steel. *ACS Omega* 8:19613–19624
21. Gouda M, Khalaf MM, Shalabi K, Al-Omair MA, Abd El-Lateef HM (2022) Synthesis and characterization of Zn-organic frameworks containing chitosan as a low-cost inhibitor for sulfuric-acid-induced steel corrosion: practical and computational exploration. *Polymers*. <https://doi.org/10.3390/polym14020228>
22. Kesari P, Udayabhanu G, Roy A, Pal S (2023) Chitosan based titanium and iron oxide hybrid bio-polymeric nanocomposites as potential corrosion inhibitor for mild steel in acidic medium. *Int J Biol Macromol* 225:1323–1349
23. Liu HL, Zhu ZM, Hu JF, Lai X, Qu JQ (2022) Inhibition of Q235 corrosion in sodium chloride solution by chitosan derivative and its synergistic effect with ZnO. *Carbohydr Polym*. <https://doi.org/10.1016/j.carbpol.2022.119936>
24. Shahini MH, Ramezanzadeh B, Mohammadloo HE (2021) Recent advances in biopolymers/carbohydrate polymers as effective corrosion inhibitive macro-molecules: a review study from experimental and theoretical views. *J Mol Liq*. <https://doi.org/10.1016/j.molliq.2020.115110>
25. Umoren PS, Kavaz D, Umoren SA (2022) Corrosion inhibition evaluation of Chitosan-CuO nanocomposite for carbon steel in 5% HCl solution and effect of KI addition. *Sustainability*. <https://doi.org/10.3390/su14137981>
26. Umoren SA, Solomon MM, Nzila A, Obot IB (2022) Corrosion inhibition of Rumex vesicarius mediated chitosan-AgNPs composite for C1018 CS in  $CO_2$ -saturated 3.5% NaCl medium under static and hydrodynamic conditions. *Sustainability* 14:1642
27. Wang LL, Han F, Zeng GP, Hu Y, Chen W, Zhang F, Song WG (2023) Excellent compound inhibitor of carboxymethyl chitosan/magnetic reduced graphene oxide for carbon steel in neutral chloride solution. *Mater Chem Phys*. <https://doi.org/10.1016/j.matchemphys.2022.126939>
28. Wu J, Wu J, Lu LL, Mei P (2023) 8-Hydroxyquinoline-functionalized chitosan Schiff base as an efficient and environmentally

friendly corrosion inhibitor for N80 steel in acidic environments. *J Appl Polym Sci.* <https://doi.org/10.1002/app.54073>

- 29. Zhang WW, Zhang YX, Li BZ, Guo HY, Dou XY, Lu K, Feng YY (2023) High-performance corrosion resistance of chemically-reinforced chitosan as ecofriendly inhibitor for mild steel. *Bioelectrochemistry.* <https://doi.org/10.1016/j.bioelechem.2022.108330>
- 30. Gawad SA, Nasr A, Fekry AM, Filippov LO (2021) Electrochemical and hydrogen evolution behaviour of a novel nano-cobalt/nano-chitosan composite coating on a surgical 316L stainless steel alloy as an implant. *Int J Hydrogen Energy.* <https://doi.org/10.1016/j.ijhydene.2021.03.018>
- 31. Szöke AF, Szabó GS, Hórvölgyi Z, Albert E, Végh AG, Zimányi L, Muresan LM (2020) Accumulation of 2-acetylaminio-5-mercapto-1,3,4-thiadiazole in chitosan coatings for improved anticorrosive effect on zinc. *Int J Biol Macromol* 142:423–431
- 32. Zheludkevich ML, Tedim J, Freire CSR, Fernandes SCM, Kallip S, Lisenkov A, Gandini A, Ferreira MGS (2011) Self-healing protective coatings with “green” chitosan based pre-layer reservoir of corrosion inhibitor. *J Mater Chem* 21:4805–4812
- 33. Aghzzaf AA, Rhouta B, Steinmetz J, Rocca E, Aranda L, Khalil A, Yvon J, Daoudi L (2012) Corrosion inhibitors based on chitosan-heptanoate modified beidellite. *Appl Clay Sci* 65–66:173–178
- 34. Bao Q, Zhang D, Wan Y (2011) 2-Mercaptobenzothiazole doped chitosan/11-alkanethiolate acid composite coating: dual function for copper protection. *Appl Surf Sci* 257:10529–10534
- 35. Cheng S, Chen S, Liu T, Chang X, Yin Y (2007) Carboxymethylchitosan as an ecofriendly inhibitor for mild steel in 1 M HCl. *Mater Lett* 61:3276–3280
- 36. Cui G, Guo J, Zhang Y, Zhao Q, Fu S, Han T, Zhang S, Wu Y (2019) Chitosan oligosaccharide derivatives as green corrosion inhibitors for P110 steel in a carbon-dioxide-saturated chloride solution. *Carbohydr Polym* 203:386–395
- 37. El-Haddad MN (2013) Chitosan as a green inhibitor for copper corrosion in acidic medium. *Int J Biol Macromol* 55:142–149
- 38. Zhao Q, Guo J, Cui G, Han T, Wu Y (2020) Chitosan derivatives as green corrosion inhibitors for P110 steel in a carbon dioxide environment. *Coll Surf B: Biointerfaces.* <https://doi.org/10.1016/j.colsurfb.2020.111150>
- 39. Verma C, Quraishi MA, Alfantazi A, Rhee KY (2021) Corrosion inhibition potential of chitosan based Schiff bases: design, performance and applications. *Int J Biol Macromol* 184:135–143
- 40. Amalraj A, Jude S, Gopi S (2020) Chapter 1—Polymer blends, composites and nanocomposites from chitin and chitosan; manufacturing, characterization and applications. In: Gopi S, Thomas S, Pius A (eds) *Handbook of chitin and chitosan*. Elsevier, Amsterdam, pp 1–46
- 41. Hasnain MS, Nayak AK (2018) 21—Chitosan as responsive polymer for drug delivery applications. In: Makhlof ASH, Abu-Thabit NY (eds) *Stimuli responsive polymeric nanocarriers for drug delivery applications*, vol 1. Woodhead Publishing, Sawston, pp 581–605
- 42. Nagasawa K, Tohira Y, Inoue Y, Tanoura N (1971) Reaction between carbohydrates and sulfuric acid: Part I. Depolymerization and sulfation of polysaccharides by sulfuric acid. *Carbohydr Res* 18:95–102
- 43. Rajeswari A, Gopi S, Jackcina Stobel Christy E, Jayaraj K, Pius A (2020) Chapter 9—Current research on the blends of chitosan as new biomaterials. In: Gopi S, Thomas S, Pius A (eds) *Handbook of chitin and chitosan*. Elsevier, Amsterdam, pp 247–283
- 44. Peter MG (1995) Applications and environmental aspects of chitin and chitosan. *J Macromol Sci Pure Appl Chem* A32:629–640
- 45. Lopes PP, Tanabe EH, Bertuol DA (2020) Chapter 13—Chitosan as biomaterial in drug delivery and tissue engineering. In: Gopi S, Thomas S, Pius A (eds) *Handbook of chitin and chitosan*. Elsevier, Amsterdam, pp 407–431
- 46. Badr EA, Hefni HHH, Shafeek SH, Shaban SM (2020) Synthesis of anionic chitosan surfactant and application in silver nanoparticles preparation and corrosion inhibition of steel. *Int J Biol Macromol* 157:187–201
- 47. Bahari HS, Ye F, Carrillo EAT, Leliopoulos C, Savaloni H, Dutta J (2020) Chitosan nanocomposite coatings with enhanced corrosion inhibition effects for copper. *Int J Biol Macromol* 162:1566–1577
- 48. Pitakchatwong C, Schlegel I, Landfester K, Crespy D, Chirachanchai S (2018) Chitosan nanocapsules for pH-triggered dual release based on corrosion inhibitors as model study. *Part Part Syst Charact.* <https://doi.org/10.1002/ppsc.201800086>
- 49. Santos LRL, Marino CEB, Riegel-Vidotti IC (2019) Silica/chitosan hybrid particles for smart release of the corrosion inhibitor benzotriazole. *Eur Polym J* 115:86–98
- 50. Li ML, Li RH, Xu J, Han X, Yao TY, Wang J (2014) Thiocarbonylhydrazide-modified chitosan as anticorrosion and metal ion adsorbent. *J Appl Polym Sci* 131:8437–8443
- 51. Li M, Xu J, Li R, Wang D, Li T, Yuan M, Wang J (2014) Simple preparation of aminothiourea-modified chitosan as corrosion inhibitor and heavy metal ion adsorbent. *J Colloid Interface Sci* 417:131–136
- 52. Mouaden KE, Chauhan DS, Quraishi MA, Bazzi L (2020) Thiocarbonylhydrazide-crosslinked chitosan as a bioinspired corrosion inhibitor for protection of stainless steel in 3.5% NaCl. *Sustain Chem Pharm.* <https://doi.org/10.1016/j.scp.2020.100213>
- 53. Chauhan DS, Srivastava V, Joshi PG, Quraishi MA (2018) PEG cross-linked chitosan: a biomacromolecule as corrosion inhibitor for sugar industry. *Int J Ind Chem* 9:363–377
- 54. Chauhan DS, Mouaden KE, Quraishi MA, Bazzi L (2020) Aminotriazolethiol-functionalized chitosan as a macromolecule-based bioinspired corrosion inhibitor for surface protection of stainless steel in 3.5% NaCl. *Int J Biol Macromol* 152:234–241
- 55. Rbaa M, Fardioui M, Verma C, Abousalem AS, Galai M, Ebenso EE, Guedira T, Lakhrissi B, Warad I, Zarrouk A (2020) 8-hydroxyquinoline based chitosan derived carbohydrate polymer as biodegradable and sustainable acid corrosion inhibitor for mild steel: experimental and computational analyses. *Int J Biol Macromol* 155:645–655
- 56. Fekry AM, Mohamed RR (2010) Acetyl thiourea chitosan as an eco-friendly inhibitor for mild steel in sulphuric acid medium. *Electrochim Acta* 55:1933–1939
- 57. Alsabagh AM, Elsabee MZ, Moustafa YM, Elsky A, Morsi RE (2014) Corrosion inhibition efficiency of some hydrophobically modified chitosan surfactants in relation to their surface active properties. *Egypt J Pet* 23:349–359
- 58. Eduok U, Ohaeri E, Szpunar J (2018) Electrochemical and surface analyses of X70 steel corrosion in simulated acid pickling medium: effect of poly (N-vinyl imidazole) grafted carboxymethyl chitosan additive. *Electrochim Acta* 278:302–312
- 59. Eduok U, Ohaeri E, Szpunar J (2019) Conversion of imidazole to N-(3-aminopropyl)imidazole toward enhanced corrosion protection of steel in combination with carboxymethyl chitosan grafted poly(2-methyl-1-vinylimidazole). *Ind Eng Chem Res* 58:7179–7192
- 60. Darmokoesoemo H, Suyanto S, Anggara LS, Amenaghawon AN, Kusuma HS (2018) Application of carboxymethyl chitosan-benzaldehyde as anticorrosion agent on steel. *Int J Chem Eng.* <https://doi.org/10.1155/2018/4397867>
- 61. Erna M, Herdini H, Futra D (2019) Corrosion inhibition mechanism of mild steel by amylose-acetate/carboxymethyl chitosan composites in acidic media. *Int J Chem Eng.* <https://doi.org/10.1155/2019/8514132>
- 62. Macedo RGMDA, Marques NDN, Tonholo J, Balaban RDC (2019) Water-soluble carboxymethylchitosan used as corrosion

inhibitor for carbon steel in saline medium. *Carbohydr Polym* 205:371–376

63. Liu Y, Zou C, Yan X, Xiao R, Wang T, Li M (2015)  $\beta$ -cyclodextrin modified natural chitosan as a green inhibitor for carbon steel in acid solutions. *Ind Eng Chem Res* 54:5664–5672

64. Lai X, Hu J, Ruan T, Zhou J, Qu J (2021) Chitosan derivative corrosion inhibitor for aluminum alloy in sodium chloride solution: a green organic/inorganic hybrid. *Carbohydr Polym*. <https://doi.org/10.1016/j.carbpol.2021.118074>

65. John S, Salam A, Baby AM, Joseph A (2019) Corrosion inhibition of mild steel using chitosan /  $TiO_2$  nanocomposite coatings. *Prog Org Coat* 129:254–259

66. Rbaa M, Benhiba F, Hssisou R, Lakhrissi Y, Lakhrissi B, Touhami ME, Warad I, Zarrouk A (2021) Green synthesis of novel carbohydrate polymer chitosan oligosaccharide grafted on D-glucose derivative as bio-based corrosion inhibitor. *J Mol Liq*. <https://doi.org/10.1016/j.molliq.2020.114549>

67. Höhlinger M, Christa D, Zimmermann V, Heise S, Boccaccini AR, Virtanen S (2019) Influence of proteins on the corrosion behavior of a chitosan-bioactive glass coated magnesium alloy. *Mater Sci Eng C Mater Biol* 100:706–714

68. Wang Q, Zhang J, Shi D, Du M (2015) Synthesis, characterization and inhibition performance of vanillin-modified chitosan quaternary ammonium salts for Q235 steel corrosion in HCl solution. *J Surfactants Deterg* 18:825–835

69. Quraishi MA, Ansari KR, Chauhan DS, Umores SA, Mazumder MAJ (2020) Vanillin modified chitosan as a new bio-inspired corrosion inhibitor for carbon steel in oil-well acidizing relevant to petroleum industry. *Cellulose* 27:6425–6443

70. John S, Joseph A, Kuruvilla M, Sajini S (2017) Inhibition of mild steel corrosion using chitosan-polyvinyl alcohol nanocomposite films by sol-gel method: an environmentally friendly approach. *J Bio-Tribio-Corr* 3:3

71. Hassannejad H, Nouri A, Soltani S, Molavi FK (2019) Study of corrosion behavior of the biodegradable chitosan-polyvinyl alcohol coatings on AA8011 aluminum alloy. *Mater Res Express*. <https://doi.org/10.1088/2053-1591/ab0432>

72. Ansari KR, Chauhan DS, Quraishi MA, Mazumder MAJ, Singh A (2020) Chitosan Schiff base: an environmentally benign biological macromolecule as a new corrosion inhibitor for oil & gas industries. *Int J Biol Macromol* 144:305–315

73. Menaka R, Subhashini S (2016) Chitosan Schiff base as eco-friendly inhibitor for mild steel corrosion in 1 M HCl. *J Adhes Sci Technol* 30:1622–1640

74. Menaka R, Subhashini S (2017) Chitosan schiff base as effective corrosion inhibitor for mild steel in acid medium. *Polym Int* 66:349–358

75. Menaka R, Geethanjali R, Subhashini S (2018) Electrochemical investigation of eco-friendly chitosan schiff base for corrosion inhibition of mild steel in acid medium. *Mater Today: Proc* 5:16617–16625

76. Chen NL, Kong PP, Feng HX, Wang YY, Bai DZ (2019) Corrosion mitigation of chitosan Schiff base for Q235 steel in 1.0 M HCl. *J Bio Tribio-Corros*. <https://doi.org/10.1007/s40735-019-019-019-7>

77. Kong P, Chen N, Lu Y, Feng H, Qiu J (2019) Corrosion by polyaniline/salicylaldehyde modified chitosan in hydrochloric acid solution. *Int J Electrochem Sci* 14:9774–9775

78. Kong P, Feng H, Chen N, Lu Y, Li S, Wang P (2019) Polyaniline/chitosan as a corrosion inhibitor for mild steel in acidic medium. *RSC Adv* 9:9211–9217

79. Jessima SJHM, Subhashini S, Berisha A, Oral A, Srikanth SS (2021) Corrosion mitigation performance of disodium EDTA functionalized chitosan biomacromolecule - experimental and theoretical approach. *Int J Biol Macromol* 178:477–491

80. Jessima SJHM, Berisha A, Srikanth SS, Subhashini S (2020) Preparation, characterization, and evaluation of corrosion inhibition efficiency of sodium lauryl sulfate modified chitosan for mild steel in the acid pickling process. *J Mol Liq*. <https://doi.org/10.1016/j.molliq.2020.114382>

81. Li P, He L, Li X, Liu X, Sun M (2021) Corrosion inhibition effect of N-(4-diethylaminobenzyl) quaternary ammonium chitosan for X80 pipeline steel in hydrochloric acid solution. *Int J Electrochem Sci* 16:1–21

82. Rasheed PA, Pandey RP, Jabbar KA, Samara A, Abdullah AM, Mahmoud KA (2020) Chitosan/lignosulfonate nanospheres as “green” biocide for controlling the microbiologically influenced corrosion of carbon steel. *Materials*. <https://doi.org/10.3390/ma13112484>

83. Farhadian A, Varfolomeev MA, Shaabani A, Nasiri S, Vakhitov I, Zaripova YF, Yarkovoi VV, Sukhov AV (2020) Sulfonated chitosan as green and high cloud point kinetic methane hydrate and corrosion inhibitor: experimental and theoretical studies. *Carbohydr Polym*. <https://doi.org/10.1016/j.carbpol.2020.116035>

84. Jia Z, Xiong P, Shi Y, Zhou W, Cheng Y, Zheng Y, Xi T, Wei S (2016) Inhibitor encapsulated, self-healable and cytocompatible chitosan multilayer coating on biodegradable Mg alloy: a pH-responsive design. *J Mater Chem B Mater Biol Med* 4:2498–2511

85. Song J, Cui X, Jin G, Cai Z, Liu E, Li X, Chen Y, Lu B (2018) Self-healing conversion coating with gelatin–chitosan microcapsules containing inhibitor on AZ91D alloy. *Surf Eng* 34:79–84

86. El-Mahdy GA, Atta AM, Al-Lohedan HA, Ezzat AO (2015) Influence of green corrosion inhibitor based on chitosan ionic liquid on the steel corrodibility in chloride solution. *Int J Electrochem Sci* 10:5812–5826

87. Zheng Y, Gao Y, Li H, Yan M, Guo R, Liu Z (2021) Corrosion inhibition performance of composite based on chitosan derivative. *J Mol Liq*. <https://doi.org/10.1016/j.molliq.2020.114679>

88. Chen T, Zeng D, Zhou S (2018) Study of polyaspartic acid and chitosan complex corrosion inhibition and mechanisms. *Pol J Environ Stud* 27:1441–1448

89. Zeng D, Chen T, Zhou S (2015) Synthesis of polyaspartic acid/chitosan graft copolymer and evaluation of its scale inhibition and corrosion inhibition performance. *Int J Electrochem Sci* 10:9513–9527

90. Sangeetha Y, Meenakshi S, Sundaram CS (2016) Interactions at the mild steel acid solution interface in the presence of O-fumaryl-chitosan: electrochemical and surface studies. *Carbohydr Polym* 136:38–45

91. Wan K, Feng P, Hou B, Li Y (2016) Enhanced corrosion inhibition properties of carboxymethyl hydroxypropyl chitosan for mild steel in 1.0 M HCl solution. *RSC Adv* 6:77515–77524

92. Wang C, Chen J, Hu B, Liu Z, Wang C, Han J, Su M, Li Y, Li C (2019) Modified chitosan-oligosaccharide and sodium silicate as efficient sustainable inhibitor for carbon steel against chloride-induced corrosion. *J Clean Prod*. <https://doi.org/10.1016/j.jclepro.2019.117823>

93. Sangeetha Y, Meenakshi S, Sairam Sundaram C (2015) Corrosion mitigation of N-(2-hydroxy-3-trimethyl ammonium)propyl chitosan chloride as inhibitor on mild steel. *Int J Biol Macromol* 72:1244–1249

94. Yang XH, Liao SQ, Liao JH (2007) Study on corrosion inhibition of chitosan quaternary ammonium for carbon steel in sulfuric acid. *Corros Sci Prot Technol* 19:255–258

95. Zanca C, Mendolia I, Capuana E, Blanda G, Pavia FC, Brucato V, Ghersi G, La Carrubba V, Piazza S, Sunseri C, Inguanta R (2019) Co-deposition and characterization of hydroxyapatite-chitosan and hydroxyapatite-polyvinylacetate coatings on 304 SS for biomedical devices, *Key Engineering Materials*, pp 153–158

96. Hefni HHH, Azzam EM, Badr EA, Hussein M, Tawfik SM (2016) Synthesis, characterization and anticorrosion potentials

of chitosan-g-PEG assembled on silver nanoparticles. *Int J Biol Macromol* 83:297–305

97. Eeduok U, Ohaeri E, Szpunar J, Akpan I (2020) Synthesis, characterization and application of glucosyloxyethyl acrylate graft chitosan against pipeline steel corrosion. *J Mol Liq.* <https://doi.org/10.1016/j.molliq.2020.113772>

98. Wang M, Zhang J, Wang Q, Du M (2019) Synthesis, characterization and corrosion inhibition performance of the thiourea-chitosan in acidic medium. *Int J Electrochem Sci* 14:8852–8868

99. Zhang QH, Hou BS, Li YY, Zhu GY, Liu HF, Zhang GA (2020) Two novel chitosan derivatives as high efficient eco-friendly inhibitors for the corrosion of mild steel in acidic solution. *Corros Sci.* <https://doi.org/10.1016/j.corsci.2019.108346>

100. Keerthana AK, Ashraf PM (2020) Carbon nanodots synthesized from chitosan and its application as a corrosion inhibitor in boat-building carbon steel BIS2062. *Appl Nanosci (Switzerland)* 10:1061–1071

101. Carneiro J, Tedim J, Fernandes SCM, Freire CSR, Gandini A, Ferreira MGS, Zheludkevich ML (2013) Chitosan as a smart coating for controlled release of corrosion inhibitor 2-mercapto-benzothiazole. *ECS Electrochem Lett* 2:C19–C22

102. Srivastava M, Srivastava SK, Nikhil JG, Prakash R (2019) Chitosan based new nanocomposites for corrosion protection of mild steel in aggressive chloride media. *Int J Biol Macromol* 140:177–187

103. Carneiro J, Tedim J, Fernandes SCM, Freire CSR, Silvestre AJD, Gandini A, Ferreira MGS, Zheludkevich ML (2012) Chitosan-based self-healing protective coatings doped with cerium nitrate for corrosion protection of aluminum alloy 2024. *Prog Org Coat* 75:8–13

104. Carneiro J, Tedim J, Fernandes SCM, Freire CSR, Gandini A, Ferreira MGS, Zheludkevich ML (2013) Functionalized chitosan-based coatings for active corrosion protection. *Surf Coat Technol* 226:51–59

105. Yavari Z, Nematian S, Saraveni H, Noroozifar M (2020) A simple strategy to increase inhibitory activity of chitosan towards iron corrosion in acidic media. *Indian J Chem Technol* 27:227–234

106. Gupta NK, Joshi PG, Srivastava V, Quraishi MA (2018) Chitosan: a macromolecule as green corrosion inhibitor for mild steel in sulfamic acid useful for sugar industry. *Int J Biol Macromol* 106:704–711

107. Solomon MM, Gerengi H, Kaya T, Kaya E, Umuren SA. 2017. Synergistic inhibition of St37 steel corrosion in 15%  $H_2SO_4$  solution by chitosan and iodide ion additives. *Cellulose* 2(2):931–950

108. Li YT, Shao LY, Wu MT, Liu JG (2009) Inhibition behavior of water soluble chitosan compounds with other inhibitive components. *Corros Prot* 30:161–164

109. Szőke ÁF, Szabó GS, Hórvölgyi Z, Albert E, Gaina L, Muresan LM (2019) Eco-friendly indigo carmine-loaded chitosan coatings for improved anti-corrosion protection of zinc substrates. *Carbohydr Polym* 215:63–72

110. De Sousa LL, Ricci VP, Prado DG, Apolinario RC, De Oliveira Vercik LC, Da Silva Rigo EC, Dos Santos Fernandes MC, Mariano NA (2017) Titanium coating with hydroxyapatite and chitosan doped with silver nitrate. *Mater Res* 20:863–868

111. Fayomi OSI, Akande IG, Oluwole OO, Daramola D (2018) Effect of water-soluble chitosan on the electrochemical corrosion behaviour of mild steel. *Chem Data Collect* 17–18:321–326

112. Nu’aim Razali N, Jain Kassim M, Hazwan Hussin M, Hazwani Dahon N, Kang Wei T (2010) A study of corrosion inhibitor of mild steel by carboxymethylchitosan in 1 M HCl. *J Corros Sci Eng* 13

113. Sun H, Wang H, Wang H, Yan Q (2018) Enhanced removal of heavy metals from electroplating wastewater through electrocoagulation using carboxymethyl chitosan as corrosion inhibitor for steel anode. *Environ Sci Water Res Technol* 4:1105–1113

114. Oh SJ, Cook DC, Townsend HE (1998) Characterization of iron oxides commonly formed as corrosion products on steel. *Hyperfine Interact* 112:59–65

115. Brou YS, Coulibaly NH, Diki NGYS, Creus J, Trokourey A (2020) Chitosan biopolymer effect on copper corrosion in 3.5 wt.% NaCl solution: electrochemical and quantum chemical studies. *Int J Corros Scale Inhib* 9:182–200

116. Fayomi OSI, Akande IG, Popoola API (2018) Corrosion protection effect of chitosan on the performance characteristics of A6063 alloy. *J Bio- Tribo-Corros.* <https://doi.org/10.1007/s40735-018-0192-6>

117. Oukhrib R, El Ibrahimy B, Bourzi H, El Mouaden K, Jmiai A, El Issami S, Bammou L, Bazzi L (2017) Quantum chemical calculations and corrosion inhibition efficiency of biopolymer “chitosan” on copper surface in 3%NaCl. *J Mater Environ Sci* 8:195–208

118. Yang SF, Wen Y, Yi P, Xiao K, Dong CF (2017) Effects of chitosan inhibitor on the electrochemical corrosion behavior of 2205 duplex stainless steel. *Int J Miner Metall Mater.* <https://doi.org/10.1007/s12613-017-1518>

119. Jmiai A, El Ibrahimy B, Tara A, Oukhrib R, El Issami S, Jbara O, Bazzi L, Hilali M (2017) Chitosan as an eco-friendly inhibitor for copper corrosion in acidic medium: protocol and characterization. *Cellulose* 24:3843–3867

120. Awaliah TP, Asnawati D, Hamdiani S (2020) Effectivity of water-soluble chitosan from rajungan shell waste as corrosion inhibitor on iron in 1 M HCl. *J Phys: Conf Ser.* <https://doi.org/10.1088/1742-6596/1594/1/012004>

121. Abdallah M, Fawzy A, Hawsawi H (2020) Maltodextrin and chitosan polymers as inhibitors for the corrosion of carbon steel in 1.0 M hydrochloric acid. *Int J Electrochem Sci* 15:5650–5663

122. Rabizadeh T, Khameneh Asl S (2019) Chitosan as a green inhibitor for mild steel corrosion: thermodynamic and electrochemical evaluations. *Mater Corros* 70:738–748

123. Safari R, Ehsani A, Kashi AH, Hadi H, Beladi FS (2021) External electric field effects on electronic properties of a candidate eco-friendly biopolymer and its anticorrosive properties in acidic media. *J Mater Eng Perform* 30:522–534

124. Mouaden K, El Ibrahimy B, Oukhrib R, Bazzi L, Hammouti B, Jbara O, Tara A, Chauhan DS, Quraishi MA. 2018. Chitosan polymer as a green corrosion inhibitor for copper in sulfide-containing synthetic seawater. *Int J Biol Macromol* 119:1311–1323

125. Eddib A, Albrimi YA, Addi AA, Douch J, Souto RM, Hamdani M (2012) Inhibitory action of non toxic compounds on the corrosion behaviour of 316 austenitic stainless steel in hydrochloric acid solution: comparison of chitosan and cyclodextrin. *Int J Electrochem Sci* 7:6599–6610

126. Bockris JOM, Reddy AKN, Gamboa-Aldeco M (2000) Modern electrochemistry 2A: fundamentals of electroics. Springer, New York

127. Revie RW, Uhlig HH (2008) Electrochemical mechanisms, corrosion and corrosion control, pp 9–19

128. Bazli L, Yusuf M, Farahani A, Kiamarzi M, Seyedhosseini Z, Nezhadmansari M, Aliasghari M, Iranpoor M (2020) Application of composite conducting polymers for improving the corrosion behavior of various substrates: a review. *J Compos Compd* 2:228–240

129. Verma C, Alfantazi A, Quraishi MA, Rhee KY (2023) Significance of Hammett and Taft substituent constants on bonding potential of organic corrosion inhibitors: tailoring of reactivity and performance. *Coord Chem Rev* 495:215385

130. Verma C, Singh A, Singh P, Yop Rhee K, Alfantazi A (2024) Regiosomeric effect of heteroatoms and functional groups of organic ligands: impacts on coordination bonding and corrosion protection performance. *Coord Chem Rev* 515:215966

131. Rinaudo M (2006) Chitin and chitosan: properties and applications. *Prog Polym Sci* 31:603–632

132. Kurita K (2001) Controlled functionalization of the polysaccharide chitin. *Prog Polym Sci* 26:1921–1971

**Publisher's Note** Springer Nature remains neutral with regard to jurisdictional claims in published maps and institutional affiliations.